



**Identification of accessible and closed substrate binding sites in the outward open cleft
of rat Organic Cation Transporter 1 (rOCT1)**

**Identifizierung von zugänglichen und unzugänglichen Substratbindungsstellen in der
nach außen offenen Konformation des organischen Kationentransporters rOCT1**

Doctoral thesis
Graduate School of Life Sciences
Julius-Maximilians-Universität, Würzburg
Section: Biomedicine

Submitted by

Saba Rehman

from

New Delhi, India

Würzburg, 2017



Submitted on:

.....

Office stamp

Members of the *Promotionskomitee*:

Chairperson:

Primary Supervisor: Prof. Dr. Hermann Koepsell

Supervisor (Second): Prof. Dr. Thomas Müller

Supervisor (Third): Prof. Dr. Erhard Wischmeyer

Date of Public Defence:

Date of Receipt of Certificates:

Contents

1 Introduction	1
1.1. SLC22 Family of Transporters	2
1.2. Organic Cation Transporters (OCTs)	4
1.1.1 Tissue distribution and sub-cellular localization	4
1.1.2 Structural characteristics	5
1.1.3 Functional characteristics	5
1.1.4 Substrate and inhibitor specificities	6
1.1.5 Clinical relevance	7
1.1.6 Mechanism of transport	8
1.1.7 Mapping of substrate-binding regions of rOCT1	9
2 Aim of the Study	13
3 Materials and Methods.....	14
3.1 Materials	14
3.1.1 Chemicals	14
3.1.2 Radioactive compounds	14
3.1.3 Cell lines	14
3.1.4 Equipments	14
3.1.5 Special reagents	14
3.1.6 Software	15
3.2 Methods	16
3.2.1 Cloning and site-directed mutagenesis of rOCT1 mutants	16
3.2.2 Expression and analysis of rOCT1 wild-type/mutants in HEK293 cells	16
3.2.2.1 Maintenance of cell culture	16
3.2.2.2 Creation of HEK293 stable cell lines	17
3.2.2.3 Binding assay in HEK293 cells	17

Table of Contents

3.2.2.4	Scintillation counting	18
3.2.2.5	Protein estimation of cell sample	18
3.2.2.6	Calculation and statistics	19
4	Results	20
4.1	[³ H]MPP ⁺ Binding	20
4.1.1	Optimization of binding measurements and binding of [³ H]MPP ⁺ to rOCT1 wild-type expressed in HEK293 cells	20
4.1.2	Binding of [³ H]MPP ⁺ to rOCT1 mutants expressed in HEK293	24
4.2	[¹⁴ C]TEA ⁺ Binding	28
4.2.1	[¹⁴ C]TEA ⁺ binding to rOCT1 wild-type expressed in HEK293	28
4.2.2	[¹⁴ C]TEA ⁺ binding to rOCT1 mutants expressed in HEK293	29
4.2.3	[¹⁴ C]TEA ⁺ binding to rOCT1 wild-type expressed in HEK293 measured in K ⁺ -phosphate buffer	31
4.3	Substrate binding inhibition studies at 0°C	32
4.3.1	[³ H]MPP ⁺ binding to rOCT1 wild-type in the presence of non-radioactive TEA ⁺ at 0°C	33
4.3.2	[¹⁴ C]TEA ⁺ binding to rOCT1 wild-type and mutant D475E in the presence of non-radioactive MPP ⁺ at 0°C	34
5	Discussion	35
6	Summary	45
7	Zusammenfassung	46
8	List of Abbreviations	48
9	References	50
10	Acknowledgements	61
11	Curriculum Vitae	63
12	List of Publications	64

Table of Contents

13 Participation in International Scientific Conferences	65
14 Affidavit/Eidesstattliche Erklärung	66

1. Introduction

A wide variety of cell transporters are present in our tissues throughout our body. They are responsible for the uptake as well as the efflux of various endogenous and exogenous compounds. These compounds are mostly hydrophilic owing to the hydrophobic nature of the plasma membrane but may include slightly hydrophobic substances as well. Of particular interest are the exogenously delivered drugs in various therapies and their products that are a result of cellular metabolism. Their effectiveness in the treatment process is mainly dependent on their concentration in blood which in turn is regulated by the drug transporters present particularly in liver, kidney, small intestine and the blood-brain barrier. A detailed knowledge of their structural and functional characteristics is therefore very important in the process of drug development. Improvements in biotechnology, *in vitro* studies in cell lines that express specific transporters stably or transiently and *in vivo* studies in animal models have increased our understanding of the structure and function of these transporters to a large extent. Besides, modern crystallization studies and protein homology modeling techniques have worked wonders in this regard.

These drug transporters can be grouped into two families based on the mechanism of their transport:

a) ATP - binding cassette (ABC) transporters

The transporters belonging to this category require ATP hydrolysis for the transport of substrates across membranes. The name of the family is derived from the ATP - binding domain found on the transporter. The involvement of ATP makes these transporters primary active. Most common examples of ABC transporters are multi-drug resistance protein (MDR), multi-drug-resistance associated protein (MRP) and the breast cancer resistance protein (BCRP).

b) Solute carrier (SLC) transporters

This group of transporters does not utilize ATP for transport as they don't have any ATP - binding sites and can be subdivided into the secondary active transporters and the facilitated transporters. The former utilize the ion gradients such as a sodium or proton gradient produced by the primary active transporters across the plasma membrane whereas the latter depend upon the electrochemical potential difference of their substrate to facilitate its transport across the membrane. A further classification of this group is also based upon the number of substrate molecules being transported and the direction of transport. A uniporter transports a single solute

molecule in one direction only; a symporter carries two solute molecules in the same direction and an anti-porter transfers two solute molecules in opposite directions.

1.1 SLC22 family of transporters

The family was named after the official gene symbol given by the Human Genome Nomenclature Committee. Based on phylogenetic similarity and preferential substrate selectivity, the known transporters of mammalian origin in this group have been subdivided into three groups (*Fig.1*) (*Koepsell 2011; Koepsell et al. 2011; Burckhardt et al. 2000*):

1. Organic cation transporters (OCTs) consist of OCT1 (*SLC22A1*), OCT2 (*SLC22A2*) and OCT3 (*SLC22A3*). The members of this group use passive diffusion for transport.
2. Organic cation/zwitterion transporters (OCTNs), consists of Na⁺-ergothioneine co-transporter OCTN1 (*SLC22A4*), Na⁺-carnitine co-transporter OCTN2 (*SLC22A5*), a mouse-specific transporter mOCTN3 (mouse *Slc22a21*) and carnitine and cation transporter OCT6 (*SLC22A16*). OCTN1 transports carnitine and also works as a proton-organic cation exchanger. OCTN2 (*SLC22A5*) functions as a Na⁺-independent transporter for organic cations. OCT6 is involved in carnitine Na⁺-independent uptake.
3. The subgroup of organic anion transporters (OATs) contains OAT1-3 (*SLC22A6-8*), human OAT4 (*SLC22A11*), urate transporter URAT1 (*SLC22A1*), rodent OAT5 (*Slc22a19*) and OAT6 (*Slc22a20*); most OATs operate as anion exchangers which couple efflux of intracellular dicarboxylates (e.g. α -ketoglutarate, lactate) with uptake of organic anions into the cell.

An important characteristic of most of the transporters of this family is their polyspecificity. They transport a variety of substrates with different sizes and molecular structures. Besides this, some of the ligands also act as inhibitors in these transporters. So, the transporters of *SLC22* family have a range of affinities as well as transport efficiencies for a variety of compounds (*Koepsell 2011; Koepsell et al. 2011; Nigam et al. 2007; Rizwan et al. 2007; Anzai et al. 2006*).

As far as the genetic make-up of *SLC22* family is concerned, members which are phylogenetically related (belong to the same subgroup) are encoded by genes present on the same chromosome band for example hOCT1-3 are can be found on chromosome 6q25.3, hOCTN1-2 on 5q23.3, and hOATs mainly on 11q12.3-11q13.1 (*Koepsell et al. 2003; Eraly et al.*

2003). Also, these genes occur in pairs probably for the purpose of facilitating co-regulation (Eraly et al. 2004).

Due to the high level of expression of these transporters in organs like intestine, liver and kidney, they are crucially involved in absorption and excretion of exogenous compounds like drugs used in therapies as well as endogenous compounds, specially the metabolites of these drugs. (Koepsell 2011; Koepsell et al. 2011; Sekine et al. 2006; Wright et al. 2004). Besides this, these transporters are also actively involved in the function of homeostasis throughout many organs in the body for instance, brain, lung and heart (Burckhardt et al. 2011; Zair et al. 2008; Lips et al. 2007; Taubert et al. 2007; Kusuhara et al. 2005; Schneider et al. 2005; Zwart et al. 2001).

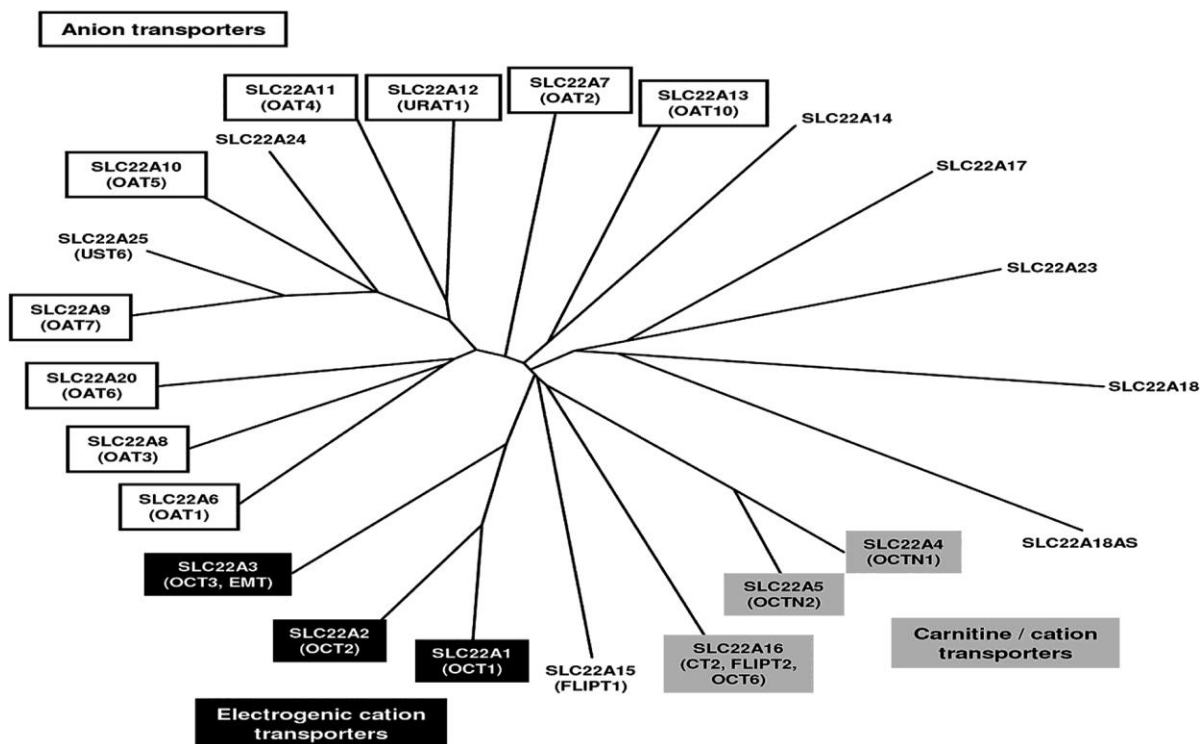


Figure 1. Phylogenetic tree of the 23 transporters of the human SLC22 family showing evolutionary relationships based on nucleotide sequences. The distance along the branches is inversely related to the sequence similarity. Electrogenic cation transporters (OCTs) are marked by black boxes, transporters for organic cations and carnitine (OCTNs) by gray boxes and transporters for organic anions (OATs) by white boxes. Transporters whose function is as yet unknown are unmarked. [Handb Exp Pharmacol (201):105-167. Copyright © 2011 Springer. Used with permission.]

1.2 Organic cation transporters (OCTs)

rOCT1 was the first transporter of this family that was identified using expression cloning of cDNA from rat kidney library in our laboratory (Koepsell et al. 2003; Gründemann et al. 1994). Next in line to be characterized was rOCT2 in 1996 (Okuda et al. 1996). rOCT3 and hOCT3 were identified two years later in 1998 (Gründemann et al. 1998; Kekuda et al. 1998).

1.2.1 Tissue distribution and sub-cellular localization

OCT1 (SLC22A1) The rat homologue of this transporter, rOCT1, is found in a variety of tissues (Koepsell et al. 2011; Koepsell et al. 2007) having strongest expression in liver, kidney and intestine (Gründemann et al. 1994). Human homologue, hOCT1, however, is mainly present in the liver (Koepsell et al. 2011, Nies et al. 2009; Jung et al. 2008; Nishimura et al. 2005; Gorboulev et al. 1997). Within the hepatocytes the expression of this transporter is mainly on the basolateral side of the hepatocytes in both rats and humans (Nies et al. 2008; Meyer-Wentrup et al. 1998). This position allows it to take in substrates brought in the liver by the blood, thus initiating the excretion process of many drugs which are cationic in nature. Apart from this, human OCT1 has been located in small amounts in a number of other tissues of the body, for example, the apical membrane of enterocytes (Koepsell 2015; Han TK et al., 2013), the apical membrane of ciliated cells in the lung (Lips et al. 2005) and of tubule epithelial cells in the kidney (Tzvetkov et al. 2009).

OCT2 (SLC22A2) The highest level of expression of hOCT2 is found in the kidney (Koepsell et al. 2011; Jung et al. 2008; Nishimura et al. 2005; Gorboulev et al. 1997), where the protein expression has been detected in the basolateral membrane of the epithelial cells of the proximal convoluted tubule (Koepsell et al. 2011; Nies et al. 2008; Motohashi et al. 2002). Just like the role that OCT1 plays in the hepatocytes, OCT2 aids in the secretion of organic cations in the kidney. It mediates the transport of these cations into the epithelial cells from the blood across the basolateral membrane. OCT2 protein has also been discovered in several other human organs, including small intestine, lung and different brain regions, and the inner ear (Koepsell et al. 2011; Ciarimboli et al. 2010; Taubert et al. 2007; Lips et al. 2005; Busch et al. 1998; Gorboulev et al. 1997). The location of hOCT2 protein is mainly apical in the ciliated epithelial cells of the lung (Koepsell et al. 2011; Lips et al. 2005) and in pyramidal cells of the hippocampus (Koepsell et al. 2011; Busch et al. 1998).

OCT3 (SLC22A3) Human OCT3 was first cloned from a kidney-derived cell line and was initially named the extraneuronal monoamine transporter (EMT) because its substrate specificity was found to be similar to monoamine uptake measured in extraneuronal tissues, neuronal expression of OCT3 was not established, and it was not known that monoamines are also transported by OCT3 (Koepsell et al. 2011; Koepsell et al. 2003; Gründemann et al. 1998). OCT3 is very broadly distributed in tissues (Koepsell et al. 2011; Nies et al. 2009; Verhaagh et al. 1999) and the protein has been traced, among others, in placenta, adrenal gland, liver, kidney, heart, lung, brain, and intestine (Koepsell et al. 2011; Koepsell et al. 2007).

1.2.2 Structural characteristics

The membrane topology of the transporters belonging to *SLC22* family including the organic cation transporters consists of 12 α -helices spanning the plasma membrane. Both the termini (N and C) are intracellular. A large glycosylated extracellular loop is present between the trans-membrane helix (TMH) 1 and 2 and an intracellular loop between TMH 6 and 7. This intracellular loop contains many phosphorylation sites (Koepsell et al. 2007) (Fig.2).

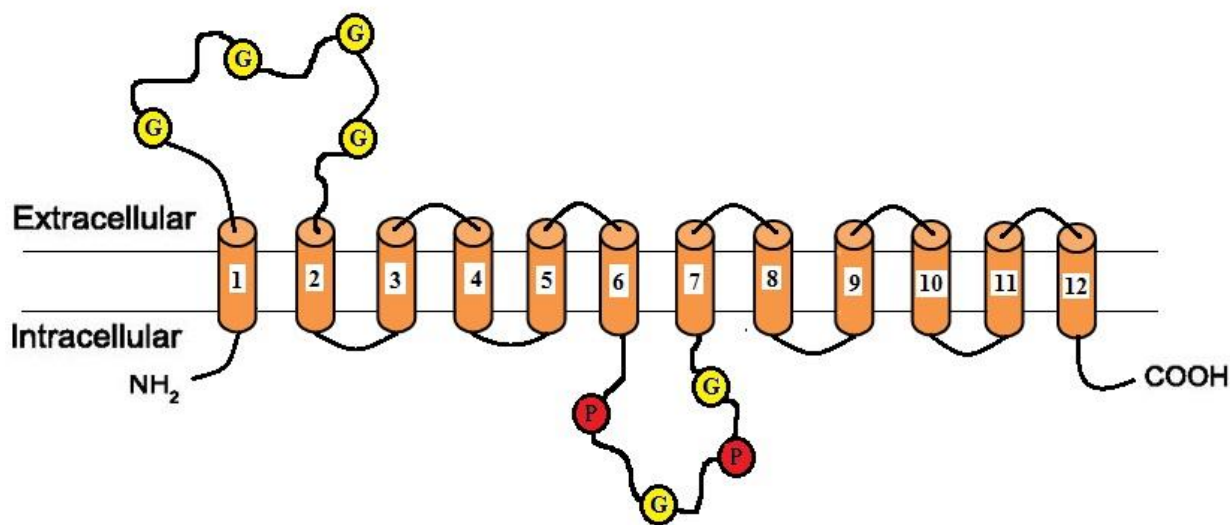


Figure 2. Predicted topology of the transporters of *SLC22* family. Predicted glycosylation sites on the large extracellular loop (G) and predicted phosphorylation sites (P) are indicated. (Image adapted from Walsh DR et. al., 2015)

1.2.3 Functional characteristics

OCT1, OCT2 and OCT3 are functionally similar in the following ways (Koepsell et al. 2007):

- a. All three are able to transport a variety of substrates and are blocked by a range of inhibitors. In other words, they are polyspecific.
- b. Most of the transported compounds belong to OCI family (<500 Da) (*Schmitt et al. 2005*).
- c. The transport is electrogenic in nature (*Arndt et al. 2001; Dresser et al. 2000; Okuda et al. 1999; Kekuda et al. 1998; Busch et al. 1998; Gorboulev et al. 1997; Nagel et al. 1997; Busch et al. 1996; Gründemann et al. 1994*).
- d. All of these transporters are Cl⁻ and Na⁺-independent and are independent of proton gradients when the effect of proton gradients on the membrane potential is excluded (*Kimura et al. 2002; Kekuda et al. 1998; Gorboulev et al. 1997; Busch et al. 1996*).
- e. OCTs are able to translocate organic cations across the plasma membrane in either direction (*Lips et al. 2005; Busch et al. 1998; Kekuda et al. 1998; Nagel et al. 1997; Busch et al. 1996*).

1.2.4 Substrate and inhibitor specificities

The substrates transported through OCTs are mostly positively charged weak bases (at pH 7.4) and organic cations but some uncharged compounds are also translocated, for e.g., cimetidine at basic (*Koepsell et al. 2011; Koepsell et al. 2007; Barendt et al. 2002*). These transported substrates are comprised of a range of substances including endogenous compounds, drugs, xenobiotics and model compounds (*Koepsell et al. 2007*). 1-Methyl-4-phenylpyridinium (MPP⁺) is a model cation that is transported by OCT1, OCT2 and OCT3 from various species and exhibits high maximal uptake rates and similar Michaelis-Menten K_m values. Certain substances act as non-transported inhibitors for OCTs for instance, cations like tetrapentylammonium, decynium 22 and disprocynium, uncharged compounds like corticosterone, deoxycorticosterone, and β-estradiol and anions like probenecid and α-ketoglutarate (*Koepsell et al. 2011; Koepsell et al. 2007*).

Despite these similarities in substrate and inhibitor specificities between the three OCTs, there are differences in specificity between subtypes (*Koepsell et al. 2007; Koepsell et al. 2003*). Some cations are transported by one OCT-transporter but act as inhibitors in another case. For example, tetrabutylammonium (TBA) is a substrate of hOCT1 and rOCT1 but inhibits rOCT1 and mOCT1 (*Volk et al. 2003; Budiman et al. 2000; Dresser et al. 2000*). Mutual inhibition is also exhibited by the transported substrates of OCTs. The degree of inhibition by a high

concentration of a given inhibitor may be total or partial. Although, this inhibition is mostly competitive, deviations have also been observed for some pairs of substrate and inhibitor (Koepsell et al. 2007).

1.2.5 Clinical relevance

Since OCTs take part in the bio-distribution of a number of important compounds, mutations in OCTs or in their regulatory proteins can affect the concentration of these compounds in vital tissues like brain and heart. There is also a possibility of severe side-effects after co-medication of some drugs owing to a difference in their comparative affinities for transport. Therefore, several studies have been done *in vitro* to check the ability of drugs to inhibit transport of the OCT drug substrates, for example, metformin or cimetidine (Koepsell et al. 2011). Drug-drug interactions involving OCTs also occur *in vivo* and may mainly affect the renal secretion of drugs that are cationic in nature (Kindla et al. 2009; Ayrton et al. 2008). For example, cimetidine decreases the renal tubular secretion of ranitidine (van Crugten et al. 1986), procainamide (Lai et al. 1988), dofetilide (Abel et al. 2000), and varenicline (Feng et al. 2008). The inhibition of metformin secretion in kidney tubules by cimetidine is attributed to OCT1 (Wang ZJ et al. 2008). OCT2 and OCT3 are inhibited directly in treatments using corticosteroids (Koepsell et al. 2004; Dresser et al. 2001). Inhibition of hOCT3 has been observed to increase the interstitial concentration of noradrenaline causing increased vasoconstriction in pulmonary arteries (Horvath et al. 2003). Similarly in the CNS inhibition of OCT2 and/or OCT3 increases interstitial neurotransmitter concentrations leading to neurological and psychiatric symptoms (Eisenhofer et al. 2001; Kimelblatt et al. 1980). The excretion of cationic drugs is also affected adversely during any renal, hepatic or systemic diseased state. For example, after partial nephrectomy in rats, OCT2 expression and in turn cimetidine excretion is reduced (Ji et al. 2002). Organic cation transport in kidney is impaired in the condition of diabetes in rats (Grover et al. 2002). A potentially lethal condition associated with mutations in OCTs is lactic acidosis (Koepsell et al. 2004). Treatment of type-II diabetes with biguanides like metformin, which is a substrate of OCTs, leads to this side-effect (Koepsell et al. 2003; Dresser et al. 2001). Metformin inhibits mitochondrial complex I in the liver that in turn decreases the production of glucose (Owen et al. 2000). However, factors like renal failure, mutated OCT2 or co-medication with inhibitors of OCT2, that impair the functioning of OCT2, result in increased inhibition of

the mitochondrial complex leading to lactic acidosis. Recently, it has also been postulated that defect in OCT1 is one of the factors that is responsible for the resistance of cancer cells during anthracycline treatment (*Andreev et. al., 2016*).

1.2.6 Mechanism of transport

The most recent view for the mechanism of transport by OCTs is that they work according to the alternating access model (*Koepsell 2011*). This model suggests a series of steps involved during the translocation of substrates across the plasma membrane, starting from binding of substrate to the transporter from the extracellular side, conformational change in the transporter leading to the transfer of substrate to the intracellular side, release of the substrate on the intracellular side and finally another conformational change reorienting the transporter such that the binding site becomes available for the substrate again on the extracellular side (*Fig.3*).

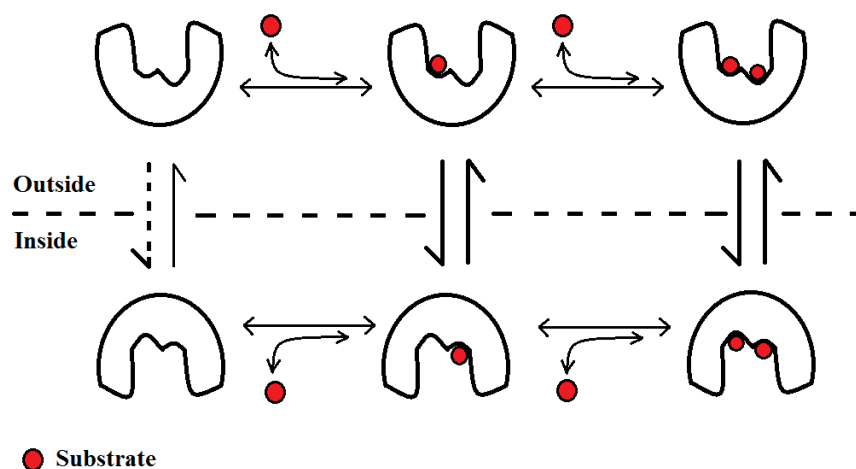


Figure 3. Alternating access mechanism of transport depicted for rOCT1

rOCT1 has been shown to possess three binding sites out of which two low-affinity binding sites are directly involved in the transport process and are indicated above whereas one high-affinity binding site is not shown. The binding of the substrate to one low-affinity binding site may alter the structure of the second one. (Image adapted from *Koepsell H., 2015*)

The evidence for this model is provided by experiments in which transport by rOCT2 was inhibited by TBuA^+ or corticosterone that was introduced in the system either from the extracellular or the intracellular side of the plasma membrane (*Volk C et. al., 2003*). The interaction of these substrates with the binding site in the outward-open conformation was established by measuring inhibition of TEA^+ induced inward-currents in intact oocytes whereas

the interaction with the binding site in the inward-open conformation was characterized by inhibition of TEA⁺ induced outward-currents in giant patches obtained from rOCT2 expressing oocytes. Corticosterone exhibited a higher affinity to the outward-open form whereas TBuA⁺ showed a higher affinity to the inward-open form of rOCT2. The data obtained through this study indicates that the substrate binding region in the cleft of rOCT2 is accessible from both sides of the membrane but with different affinities for substrates/inhibitors in the two conformations, thus supporting the alternating access mechanism.

1.2.7 Mapping of substrate binding regions of rOCT1

Site-directed mutagenesis and modeling studies have contributed immensely to the knowledge of the substrate-binding regions of rOCT1 (Koepsell 2011; Volk et al. 2009; Schmitt et al. 2009; Gorbunov et al. 2008; Popp et al. 2005). The model of inward-facing conformation of rOCT1 was based upon the crystal structure of Lactose permease *LacY* from *Escherichia coli* in the same conformation as both are members of the major facilitator superfamily (MFS) (Popp et al. 2005; Abramson et al. 2003). The model of outward-facing conformation of rOCT1 was initially made by using a presumed mechanism of rearrangement of the enzyme LacY based on biochemical data (Koepsell 2011; Volk et al. 2009; Schmitt et al. 2009; Kaback et al. 2007). However, the recent crystallization of another member of the same superfamily, Fucose transporter *FucP* also from *Escherichia coli*, in the outward-facing conformation allowed the modeling of rOCT1 on its basis in this conformation (Dang et al. 2010). Mutagenesis of rOCT1 done so far has confirmed the high quality of modeled outward- and inward-open clefts of the transporter in the following ways:

- a. Substrate selectivity and/or affinity were changed by eight mutations in the cleft region of the modeled inward-open and/or outward-open conformations (Volk et al. 2009; Gorbunov et al. 2008; Popp et al. 2005; Gorboulev et al., 2005; Gorboulev et al., 1999). These include: Phe160 on TMH 2; Trp218, Tyr222 and Thr226 on successive turns of TMH 4; Arg440, Leu447 and Glu448 on TMH 10; and Asp475 in the middle of TMH 11 (Fig.4).
- b. Docking simulations done with inhibitors corticosterone and TBuA⁺ on rOCT1 enabled the prediction of their interaction with these sites in the transporter (Volk et al. 2009; Popp et al. 2005). The docking of corticosterone with the modeled outward-open and inward-open clefts were consistent with the functional data showing an interaction with Phe160, Trp218,

Arg440 and Leu447 (Fig.4). Interaction of Asp475 with corticosterone was also predicted which was confirmed by the measurements performed with stably transfected HEK293 cells (Volk et al. 2009). Similarly, docking simulations done with TBuA⁺ along with the experimental evidence showed that it interacts with Phe160, Leu447 and Asp475 (Volk et al. 2009).

Tracer uptake and inhibition studies employing model substrates (TEA⁺ and/or MPP⁺) in the presence and absence of inhibitors have been done on a variety of rOCT1 mutants expressed in intact oocytes, to determine the K_m , V_{max} and K_i values. Initially experiments were done using long incubation times (30 or 60min) with the passively permeating inhibitors like corticosterone so that they have access to both the intracellular as well as extracellular side of the plasma membrane (Gorbunov et al. 2008; Popp et al. 2005; Gorboulev et al., 2005; Gorboulev et al., 1999). In later experiments, corticosterone was applied to both the sides of the plasma membrane separately for short incubation times and electrical measurements were done, again on oocyte system, to differentiate between their interaction with intracellular and extracellular sides and allow the identification of binding sites playing important role in the steps of transport process – binding/translocation and release of substrates (Volk et al. 2009). The following observations were made as a result of these studies:

- a. The K_m values for both TEA⁺ and MPP⁺ were changed by mutations of Trp218 and Tyr222.
- b. The mutation Asp475 to glutamate increased the affinity for TEA⁺ but did not affect the K_m for MPP⁺.
- c. Mutations at the remaining five positions, namely, Phe160, Thr226, Arg440, Leu447 and Gln448 affected only the affinity for MPP⁺.

Having identified the crucial amino acids in the cleft of the transporter interacting with the substrate, it was also important to know, specifically, in what conformation (the outward-facing or the inward-facing) this interaction occurs. For this purpose, the later experiments of checking the effect of intracellular or extracellular corticosterone on TEA⁺-induced currents were done (Koepsell 2011; Volk et al. 2009). Firstly, short incubation times were used which prevented the passive permeation of corticosterone into the oocytes and secondly, the experiments were done on an rOCT1 mutant (C451M) because it showed increased cation-induced currents without affecting the affinity for TEA⁺ or MPP⁺ (Sturm et al., 2007). As a result, positions were identified that altered the affinity of corticosterone from both extracellular as well as intracellular

side (Phe160, Trp218 and Leu447), only from extracellular side (Arg440) and only from intracellular side (Gln448).

Experiments done with rOCT1 reconstituted in nanodiscs (*T. Keller, F. Bernhard, V. Doetsch, V. Gorboulev, H. Koepsell; unpublished data*) as well as those conducted using voltage-clamp fluorometry on a fluorescent labeled rOCT1 (*Gorbunov D et. al., 2008*), both indicate the existence of three MPP⁺ binding sites/monomer of rOCT1. Two of these are low-affinity binding sites located closely in the innermost part of the cleft in the outward-open conformation of the transporter and are shown to be directly involved in the transport process whereas one is a high-affinity binding site which might affect the transport indirectly by bringing about conformational change in the transport related sites and may be of importance due to high-affinity inhibition in drug-drug interactions.

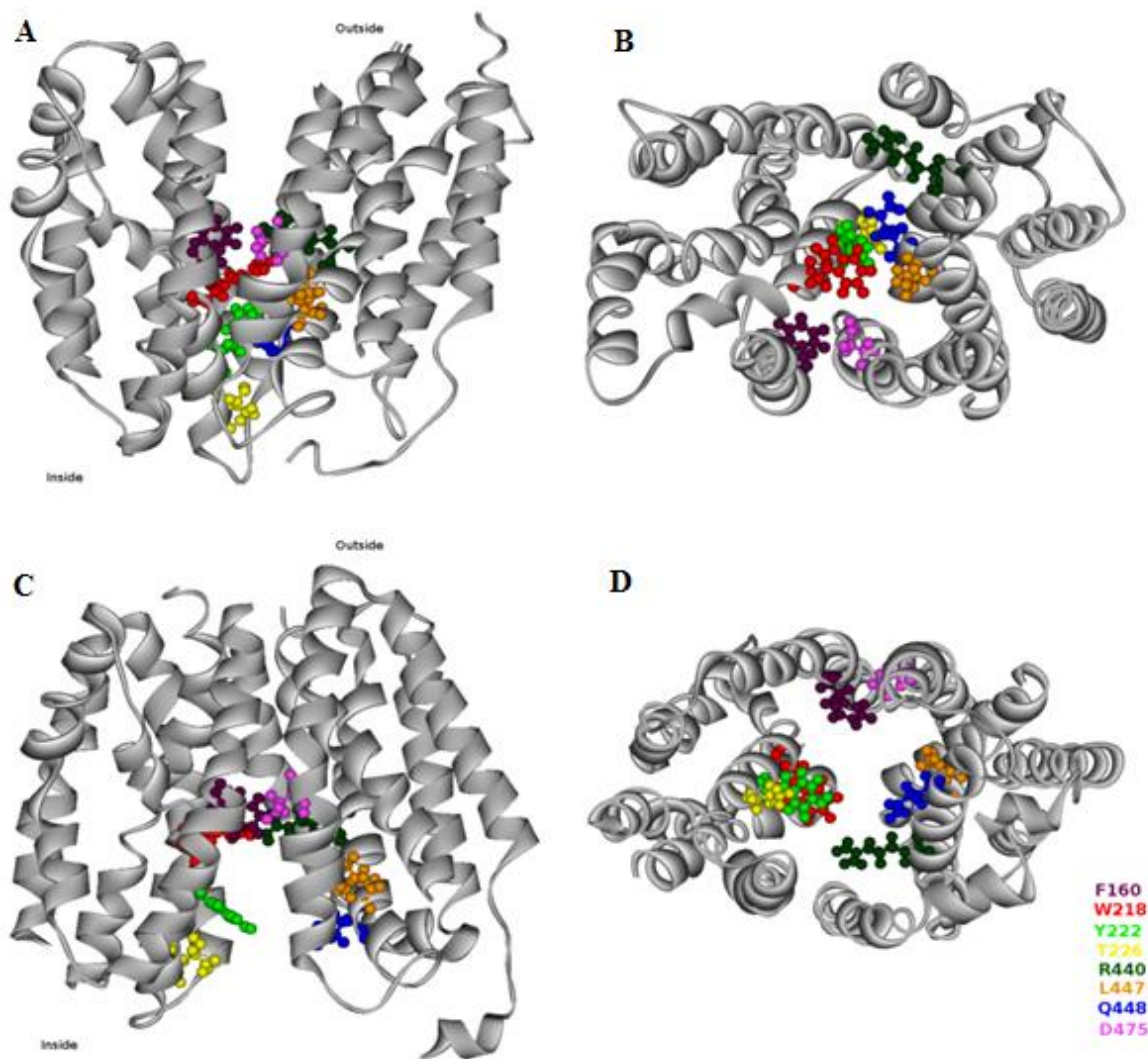


Figure 4. Structure models of rOCT1 with amino acids that are crucial for substrate affinity. Modeling of the outward- and inward-open conformation was done using tertiary structures of LacY in the outward- and inward-open conformation. Mutagenesis experiments showed that the indicated amino acids are important for affinity and/or selectivity of the substrates TEA⁺ and MPP⁺. (A) Side-view and (B) View from outside of the outward open-conformation. (C) Side-view and (D) View from inside of the inward-open conformation. (Image adapted from Koepsell H., 2011)

2. Aim of the study

The aim of this study was to further elucidate the structure of the binding site by trying to ascertain which amino acids in the binding site interact with the ligands in the outward open conformation using the tools available in the laboratory of Prof. Koepsell. The tools were stably transfected HEK293 cells expressing various mutants of rOCT1. The previous studies have helped us to identify the main amino acids in the cleft of rOCT1 that interact in a critical manner with the substrates/inhibitors either directly or indirectly. Mutations at the following sites - Trp218, Tyr222, Thr226, Leu447, Glu448 and Asp475, have been shown to have an effect on the affinities (K_m values) of MPP⁺ and TEA⁺ uptake by rOCT1 (Gorboulev *et al.*, 1999; Popp *et al.*, 2005; Gorboulev *et al.*, 2005). Also, homology modeling studies have suggested that Phe160, Trp218, Arg440, Leu447 and Asp475 interact directly with the cations (Volk *et al.*, 2009). For the present study, the following among the above mentioned sites were selected: **Asp475, Phe160, Leu447, Arg440, Trp218 and Tyr222**. Position **Lys215** was also selected as a control as it is an established non-transporting mutant. The focus was their role in substrate (specifically MPP⁺ and TEA⁺) interaction with rOCT1 for further investigating the previous observations. The approach was different from the routine uptake assays that are conducted at 37°C. This was done by measuring the dissociation constant (K_D) values of MPP⁺/TEA⁺ binding at 0°C. Since, at 37°C the transporter is in a dynamic state, it cannot be determined with surety whether these crucial amino acids in the binding site are available in the outward or inward open conformation. By bringing the temperature down to 0°C, the intention was to freeze the transporter and highlight the interaction of substrates with the prominent amino acids of the binding site in the outward open conformation. In other words, we wanted the substrate to bind but not to get translocated by the transporter in an attempt to measure binding.

3. Materials and methods

3.1. Materials

3.1.1. Chemicals

If not otherwise stated, all standard laboratory chemicals were of pro analysis (p.a.) grade and were purchased from one of the firms namely Sigma-Aldrich (Taufkirchen, Germany), Merck (Darmstadt, Germany), Perkin Elmer (Darmstadt, Germany) or AppliChem (Darmstadt, Germany). (*Minuesa et al., 2009; Arndt P et al., 2001*).

3.1.2. Radioactive compounds

[$^{14}\text{C}^+$]-Tetra-ethylammonium (TEA^+) bromide, specific activity 55mCi/mmol and [$^3\text{H}^+$]-1-Methyl-4-phenylpyridinium iodide (MPP^+), specific activity 85 Ci/mmol were purchased from Biotrend (Cologne, Germany).

3.1.3. Cell lines

- HEK293 wild-type cell line (*Graham FL et al., 1977*).

3.1.4. Equipments

- Centrifuge: Heraeus centrifuge UJ II KS
- Centrifuge: Eppendorf centrifuge 5415 C, Sigma-Aldrich (Taufkirchen, Germany)
- Thermostat ipp-400, Memmert GmbH, Germany
- Photometer Ultraspec 3, Pharmacia, Freiburg, Germany
- Liquid scintillation counter: Tri-Carb 1600CA, Packard Instrument Co., USA
- Cell Star® Cell culture flasks/plates, Greiner Bio-One (Frickenhausen, Germany).

3.1.5. Special reagents

- Lipofectamine® DNA Transfection Reagent Protocol, *Invitrogen by Life Technologies*
- Lowry solution for protein estimation: Lowry's reagent (2% sodium carbonate, 0.4% sodium hydroxide) + 0.02% potassium sodium tartarate + 0.01% copper sulphate)

3.1.6. Software

- The images of the constructed models (courtesy of Prof. Dr. Thomas Mueller) were studied and analyzed using the following software:
 - a. Discovery Studio Visualiser (*v16.1.0.15350 © 2015, Dassault Systemes Biovia Corp*)
 - b. Deep View/Swiss-PDB viewer (*v4.0.1© 1995-2000 N.Guex*)
 - c. The animated movies for presentations of transporter molecules were made using PyMol (*A molecular visualization system on an open source foundation, maintained and distributed by Schrödinger, LLC, Mannheim, Germany*)
- Statistical analyses were performed using PRISM (*GraphPad software, Inc., San Diego, Calif.*)

3.2. Methods

3.2.1. Cloning and site-directed mutagenesis of rOCT1 mutants

All constructs of rOCT1 single and double mutants used in this study were generated by Dr. Valentin Gorboulev in our lab. Most of the constructs (F160A, W218Y, W218L, R440K, L447Y, D475E and Y222F) were prepared earlier (Gorboulev *et al.*, 1999; Popp *et al.*, 2005; Gorboulev *et al.*, 2005; Volk *et al.*, 2009). The additional mutants - F160Y, L447F and W218F were made using the polymerase chain reaction (PCR) applying the overlap extension method (Ho *et al.*, 1989). All mutants were cloned at first into pRSSP vector (Busch *et al.*, 1996) and then transferred into the eukaryotic expression vectors pRcCMV or pcDNA3.1 (both from Invitrogen, Netherlands) for the expression of HEK293 cells. The exceptions were mutants F160Y and W218F which were cloned directly into eukaryotic expression vectors. For creation of eukaryotic expression constructs either the whole coding region of the mutant was re-cloned into the eukaryotic vector or the mutated fragment from the pRSSP construct was cut with restriction endonucleases and used for replacing the corresponding fragment in the wild-type rOCT1/pRcCMV.

All PCR-derived parts of the mutant constructs and cloning sites were sequenced to exclude undesired mutations and errors. Rat organic cation transporter 1 (rOCT1) was amplified by PCR from Rat liver total RNA using primers designed from the published rOCT1 Sequence: forward 5'-GCAACCCCCCCCCC3' and reverse 5'-GCCCCCCCC-3'. The PCR was digested with HindIII and XhoI and cloned into the oocyte vector pRSSP. Sequencing confirmed the absence of PCR errors.

3.2.2. Expression and analysis of rOCT1 and its mutants in HEK293 cells

3.2.2.1. Maintenance of cell culture

- Thawing of cells: DMEM (supplemented with 10% heat-inactivated FCS, 2mM L-glutamine and 100,000 units/l penicillin, 100mg/l streptomycin and 0.8g/l G418) was warmed to 37°C in a water bath. Cells in cryovial were stored in liquid nitrogen. They were thawed completely using the waterbath.

- Introduction of cells in flasks for initiating the culture: The cells from the vial were removed into 10ml fresh media in a centrifuge tube and spun at 1000 rpm (Centrifuge: JS21-JA 14 & JA 20, Beckman, Munich) for 5 min at room temperature. The supernatant was removed and 20ml of fresh media was added and the cell suspension was transferred into a 150ml flask (Cell Star® Greiner Bio-One, Frickenhausen, Germany). The flask was then kept in the humidified incubator at 37°C in 5% CO₂. The cells doubled in approximately 2 days.
- Passage of cells (subculture): Fresh media and PBS were warmed to 37°C in water bath. The old media in the flask was removed and the cells were rinsed, without detaching, with 5ml PBS at room temperature. The cells were then washed from the flask with 10ml fresh media. The cells were then divided 1:5 (for passage after 48h) into new flasks/plates, adding fresh media for a total volume of 20ml in each.

3.2.2.2. Creation of HEK293 stable cell lines

HEK293 cells were transfected with the vector pcDNA3.1 containing rOCT1 wild-type and rOCT1 mutants and selected for stably transfected cell lines as described (*Busch et al., 1996*) by Dr. Valentin Gorboulev. The cells were seeded to up to 70% confluency in a 60 mm cell culture dish. The required amount of DNA was transfected using lipofectamine as per the manufacturer's protocol. The cocktail (DNA + lipofectamine) was added to the cells and the media was changed after an incubation of about 24 h (if the cells looked fine) for efficient transfection. In case of cell toxicity the media was changed earlier (after about 10 h). After 2 days of incubation, the cells were trypsinized and transferred to a 10 cm plate and neomycin resistance selection was performed with increasing concentrations of geneticin G-418 (200-800µg/ml). The media was changed after every 72 h till the colonies started forming. At this point they were picked up separately and transferred to bigger plates and cultured as usual. The cell lines exhibiting the highest MPP⁺ uptake were selected for further studies.

3.2.2.3. Binding assay in HEK293 cells

Harvesting the cells for the assay: Three fully confluent cell-culture dishes (PS, 145/20 MM, Vents, CELLSTAR® TC, sterile) were taken for one complete experiment. After washing the cell layer with 1X PBS once at room temperature, the cells were detached using Mg-Ca-PBS (1X

phosphate-buffered saline with 0.5 mM MgCl₂ and 1 mM CaCl₂, pH 7.4) and transferred to a 50 ml falcon tube which was centrifuged for 5 min at 1000 × g (Heraeus centrifuge UJ II KS) at room temperature. The supernatant was discarded and the cell pellet was finally suspended again in Mg-Ca-PBS. 100 µl aliquots of this cell-suspension containing about 10⁷ cells were taken in 1.5 ml glass tubes.

Substrate concentrations: A total of 10 different concentrations of MPP⁺ (radioactive + non-radioactive) were prepared in ice-cold Mg-Ca-PBS for one experiment and for each concentration 4 measurements were done. The concentrations ranged from the starting value of 1.25 nM having only radioactive [³H]MPP⁺ to a final concentration of 5 mM MPP⁺ having the same amount of radioactive [³H]MPP⁺ in each but an increasing amount of non-radioactive MPP⁺.

The assay: The aliquots of cells-suspension prepared as mentioned above were pre-incubated in ice for 10 min. Then 100 µl of each of the above described substrate preparation was added to 4 of these aliquots and mixed using a vortex mixer. After 5 min incubation on ice, this mixture was transferred to 1.5 ml eppendorf tubes using plastic transfer pipettes (BRAND[®] pipette, Z331767, Sigma). It was then centrifuged for 2 min at 1,000 × g (Eppendorf centrifuge 5415 C, Sigma-Aldrich). The supernatant was carefully removed completely without disturbing the pellet using a disposable Pasteur pipette (MARI3233050, Marienfeld) attached to a pump. Any traces of radioactivity on the tube wall or in the solution surrounding the pellet was removed quickly by washing the surface of the pellet with 1 ml ice-cold 1X Mg-Ca-PBS using a pipette.

3.2.2.4. Scintillation counting

The cell pellets were solubilized by 1 h incubation with 4 M guanidine thiocyanate. After this, 1 ml of scintillation cocktail mix *LumasafeTM Plus* (*Lumac, Netherlands*) was added to each vial and it was analysed for radioactivity. The liquid scintillation counting was done using *Tricarb 1600* (*Packard-Bell, Dreieich, Germany*).

3.2.2.5. Protein estimation of cell sample

Lowry's method for protein estimation was used to measure the amount of protein in the cell extract as described previously (*Lowry et al., 1951*).

As a reference, BSA was taken in 100 μl at four different concentrations (5 μg , 10 μg , 20 μg and 40 μg). 100 μl 0.5% SDS was added to the pellet of cells (our sample) and vortexed. Afterwards, 1ml Lowry solution was added to both the sample and the controls and incubated for 10 min. Then, 100 μl of 1X Folin-Ciocalteu phenol reagent was added and vortexed. After an incubation of 30 min at room temperature, the optical density was measured by absorbance of 760nm wavelength using *Tungsten light in Pharmacia LKB Ultraspec III UV/visible scanning spectrophotometer (Pharmacia Biotech, Uppsala, Sweden)*. The plotting of graph was done using the values of optical density measured against control concentrations and the slope, $y = m(x) + c$, (where y = optical density values, x = unknown concentration and m and c are linear equation constants) was obtained. Using this slope, the sample concentration was determined in $\mu\text{g}/\mu\text{l}$.

3.2.3. Calculation and statistics

Software package Graph Pad Prism Version 4.1 (Graph Pad Software, San Diego, CA) was used to compute statistical parameters. Binding measurements in HEK293 cells were performed in at least three different experiments in which four individual measurements were performed per experimental condition. Dissociation constants (K_D) values for binding were determined by fitting Hill equation to radioactively traced MPP⁺ associated with HEK293 cells that have been corrected for nonspecific binding measured in presence of 5mM non-radioactive MPP. The presented K_D values represent means \pm S.D. which were obtained by fitting data from individual experiments. The curves in the presented figures were obtained by fitting data from compiled experiments. In the graphs individual data points are presented as mean values \pm S.E.M. When rOCT1 wild-type and/or mutants were compared within experimental series, significance of differences was determined by ANOVA using posthoc Newman-Keuls comparison. $P < 0.05$ was considered significant.

4. Results

Studies on rOCT1 with the aim of elucidating Michaelis-Menten constant (K_m values) for substrates and inhibitor affinities presented as half maximal concentrations for inhibition (IC_{50} values) have been performed so far in different expression systems ranging from oocytes where measurements were performed at room temperature to mammalian expression systems in which measurements were performed at 37°C. Although, observed changes in the K_m and IC_{50} values after mutations of individual amino acids may indicate the amino acids that interact directly with the ligands, they may also be due to indirect effects of mutations on ligand binding sites. The main focus of the present study was to elucidate the effects of mutations on the binding of substrates to rOCT1 by performing measurements at 0°C. By lowering the temperature, we wanted to avoid translocation by freezing the transporter in one conformation and check the interaction of the substrates MPP^+ and TEA^+ . Previously identified crucial amino acids (Asp475, Phe160, Leu447, Arg440, Trp218 and Tyr222), which are supposed to be located in the cleft region, were selected so that we could compare the outcome with already established results.

4.1 [3H]MPP⁺ binding

4.1.1. Optimization of binding measurements and binding of [3H]MPP⁺ to rOCT1 wild-type expressed in HEK293 cells

Trying to measure MPP^+ binding we reasoned that at 0°C when the membrane lipids are frozen no transport function should be possible. For this reason we tried to determine association of MPP^+ with rOCT1 expressed in HEK293 cells at 0°C. In all the binding measurements a series of [3H]MPP⁺ concentrations were used ranging from the primary one which consisted of only 1.25 nM radioactive MPP^+ to a final concentration of 5 mM made up of 1.25 nM radioactive MPP^+ mixed with an increasing concentrations of non-radioactive MPP^+ . The cells were first pre-incubated in ice to assure their inactive state. For simpler handling, a relatively long incubation time of 5 min with the substrate (as compared to the 1 sec incubation period during routine uptake assays) was used. In order to avoid dissociation of bound substrate, prolonged washing had to be avoided. So the washing step was reduced to a 1 sec quick surface wash. As a control experiment when the binding of [3H]MPP⁺ with and without washing with 1X PBS was

compared in HEK293 cells expressing rOCT1 wild-type considerable saturable binding was observed and the amount of bound [^3H]MPP $^+$ that could not be removed in the presence of 5 mM MPP $^+$ remained same in both the cases (Fig.5). When the HEK293 cells expressing rOCT1 were incubated for 5 min at 0°C with 1.25 nM [^3H]MPP $^+$ and the cells were washed in suspension in the presence of 1X PBS containing 5 mM MPP $^+$, no significant saturable MPP $^+$ association with the cells was detected (M. Tzvetkov and H. Koepsell, unpublished data). This is consistent for the absence of transport at 0°C but cannot be considered as unambiguous proof for binding because the intracellular MPP $^+$ content may be relatively low under equilibrium conditions after 5 min incubation and cellular efflux could be stimulated during washing with non-radioactive MPP $^+$.

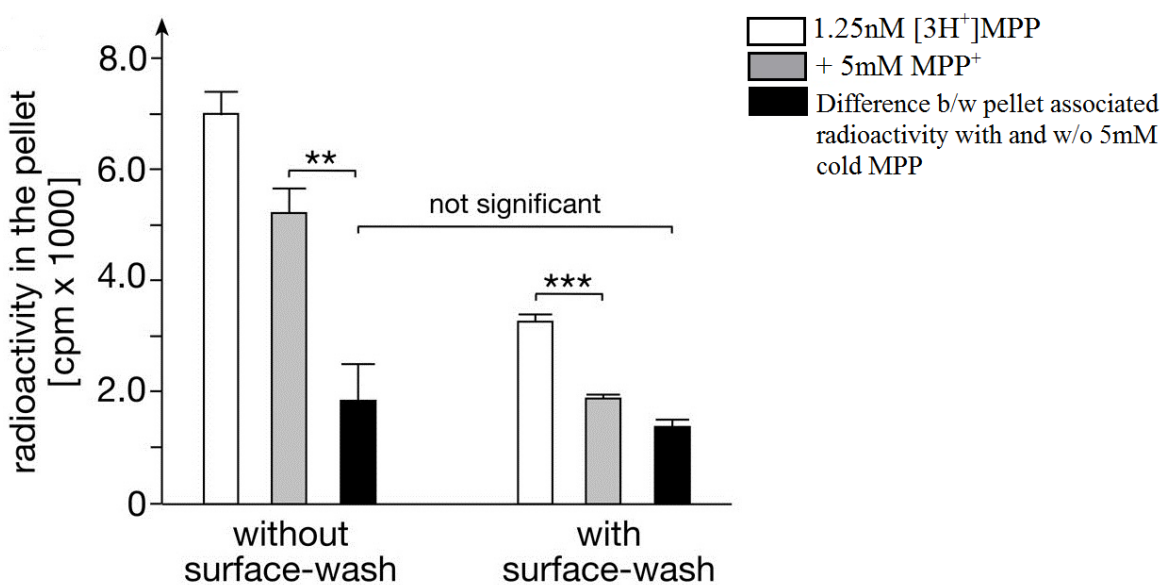


Figure 5. [^3H]MPP $^+$ binding to HEK293 cells stably transfected with rOCT1 at 0°C

HEK293 cells stably transfected with rOCT1 were incubated for 5 min at 0°C with 1.25 nM [^3H]MPP $^+$. The cells were pelleted and radioactivity in the pellet was analyzed directly after removal of the supernatant (without surface-wash) or after a quick wash of the surface of the pellet to remove any traces of radioactivity from the surface of the pellet and the tube's wall (with surface-wash). Mean values \pm S.E.M of 12 measurements from 3 independent experiments are shown. ** $P < 0.01$, *** $P < 0.001$ significance of difference determined by ANOVA with posthoc Newman-Keuls test.

In another control experiment using empty vector transfected HEK293 cells, it was observed that the degree of binding of [^3H]MPP $^+$ in presence of 5 mM non-radioactive MPP $^+$ was the same as that in HEK293 cells expressing rOCT1 wild-type (Fig.6). Therefore, the binding of [^3H]MPP $^+$ at this concentration of substrate was considered to be non-specific and thus was subtracted from the amount of binding of [^3H]MPP $^+$ in the rest of the concentration range i.e., from 1.25 nM to 500 μM [^3H]MPP $^+$ binding in all the experiments.

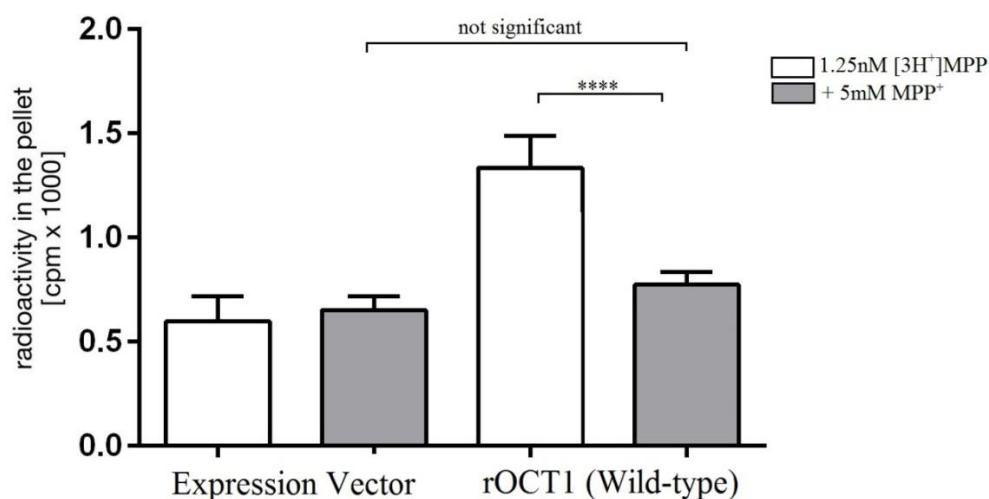


Figure 6. [^3H]MPP $^+$ binding at 0°C to HEK293 cells expressing empty vector and rOCT1 wild-type

Binding of radioactive MPP $^+$ in presence of 5mM non-radioactive MPP $^+$ was determined to be non-specific and subtracted from the MPP $^+$ binding measurements after it was found to be the same amount associated with expression vector in control experiment. Mean values \pm S.E.M of 12 measurements from 3 independent experiments are shown. **P<0.01, ****P<0.001 significance of difference determined by ANOVA with posthoc Newman-Keuls test.

HEK293 cells stably transfected with rOCT1 wild-type showed the replacement of 1.25 nM [^3H]MPP $^+$ after addition of increasing concentrations of non-radioactive MPP $^+$ thus exhibiting substrate dependence of [^3H]MPP $^+$ binding. An increase of about 20% in the amount of the bound [^3H]MPP $^+$ was observed after addition of 10 nM non-radioactive MPP $^+$ making the final MPP $^+$ concentration from 1.25 nM to 11.25 nM (Fig.7). This pointed towards the possibility of a high-affinity MPP $^+$ binding site ($K_D < 12$ nM) that allosterically induces the binding to the low-affinity binding sites. After this initial increase, a smooth replacement of bound [^3H]MPP $^+$ was observed after addition of higher concentrations till 500 μM MPP $^+$ (Fig.7). Fitting the Hill

equation to this replacement curve starting at the MPP^+ concentration of 11.25 nM (omitting the initial increase), a K_D value of $4.87 \pm 1.0 \mu M$ was obtained (Table 1). This value is nearly identical to the apparent K_m value of MPP^+ transport measured during uptake assay HEK293 cells at 37°C (H. Koepsell, V. Gorboulev and U. Roth, unpublished data). The results indicate that:

- Both the high-affinity and the low-affinity binding sites for MPP^+ are accessible to the substrate in the outward-open conformation of rOCT1
- The K_m for MPP^+ transport in our earlier experiments is determined by the binding of MPP^+ to the outward open conformation of the transporter and
- At 37°C and 0°C there is no significant difference in the structure of the low affinity MPP^+ binding site in rOCT1.

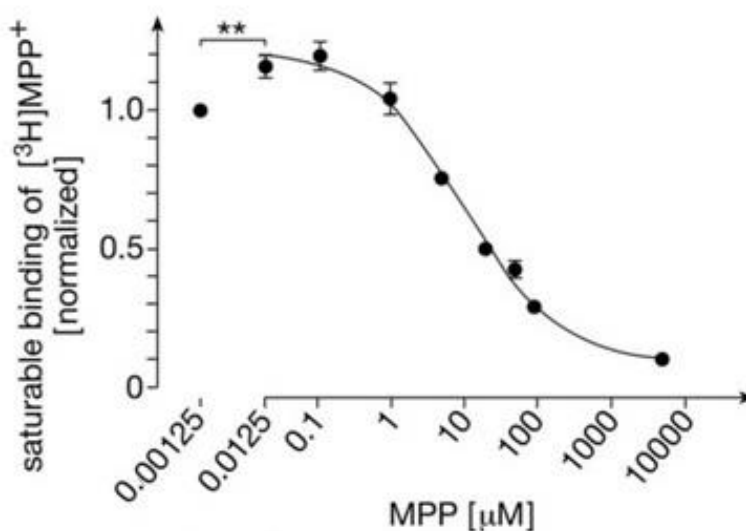


Figure 7. Concentration dependence of saturable MPP^+ binding to rOCT1 measured at 0°C. HEK293 cells stably transfected with rOCT1 were incubated for 5 min at 0°C with 1.25 nM [3H]MPP $^+$ in the presence of increasing concentrations of non-radioactive MPP^+ till a final concentration of 5 mM MPP^+ . A replacement curve showing bound [3H]MPP $^+$ in the presence of different concentrations of non-radioactive MPP^+ is plotted. The final concentration of MPP^+ is indicated on the X-axis. Mean values \pm S.E.M of 12 measurements from 3 independent experiments are indicated. The curve was obtained by fitting the Hill equation to the data starting from the values at 11.3 nM MPP^+ . * $P < 0.05$ for difference to binding measured at 1.25 nM MPP^+ was determined by Student's *t*-test.

4.1.2. Binding of [³H]MPP⁺ to rOCT1 mutants expressed in HEK293 cells

Noticeable changes in K_D value for [³H]MPP⁺ binding were observed in the mutants of rOCT1 expressed stably in HEK293 cells (*Table 1, Fig.8*). Replacement of Phe160 by alanine (F160A), led to almost a two-fold increase in the K_D for MPP⁺-binding measured at 0°C. A change in the affinity of MPP⁺-binding was also observed when Trp218 was replaced either by leucine (W218L), or by phenylalanine (W218F) or by tyrosine (W218Y). Replacement of Trp218 by leucine (W218L) and phenylalanine (W218F) led to an increase in the K_D value but no effect on the K_D for binding was seen when it was replaced by tyrosine (W218Y). When Asp475 was replaced with glutamate (D475E), a three-fold decrease in the K_D for MPP⁺-binding was observed. The K_D value remained unchanged when Tyr222 was replaced by phenylalanine (Y222F), Arg440 was replaced by lysine (R440K) and Leu447 was replaced by phenylalanine (L447F) or by tyrosine (L447Y).

Another noteworthy effect was an initial increase in binding of 1.25 nM [³H]MPP⁺ after the addition of 10 nM non-radioactive MPP⁺ in the mutants W218L and W218Y similar to the 20% increase that was observed in rOCT1 wild-type at this concentration. But in the case of these mutants (*Fig.8B*), the increase was even greater (86% in W218L and 49% in W218Y mutants). The mutations that did not have any effect on the binding of [³H]MPP⁺ to the high-affinity binding sites were F160A, Y222F, R440K and L447Y whereas the high affinity binding was completely abolished in the mutants W218F, the third mutant from the category of Trp218 mutants (*Fig.8B*) and in the mutants L447F and D475E (*Fig.8C*).

The data shows that MPP⁺ is able to interact with Phe160, Trp218 and Asp475 in the outward-open conformation. The varied effects of W218F, W218Y and D475E point towards a complicated interaction of MPP⁺ with them instead of simply being a member of low-affinity binding site in the outward-open cleft. A hint of allosteric interactions between high-affinity and low-affinity binding site is also observed due to the initial increase in MPP⁺ binding after mutations at position Trp218.

Interestingly, the already established non-transporting mutant, K215R, showed some degree of binding with a very high K_D value of $60.2 \pm 9.3 \mu\text{M}$ (*Fig.9*), supporting the presumption that the substrate binding rather than the transport was measured in our experiments at 0°C.

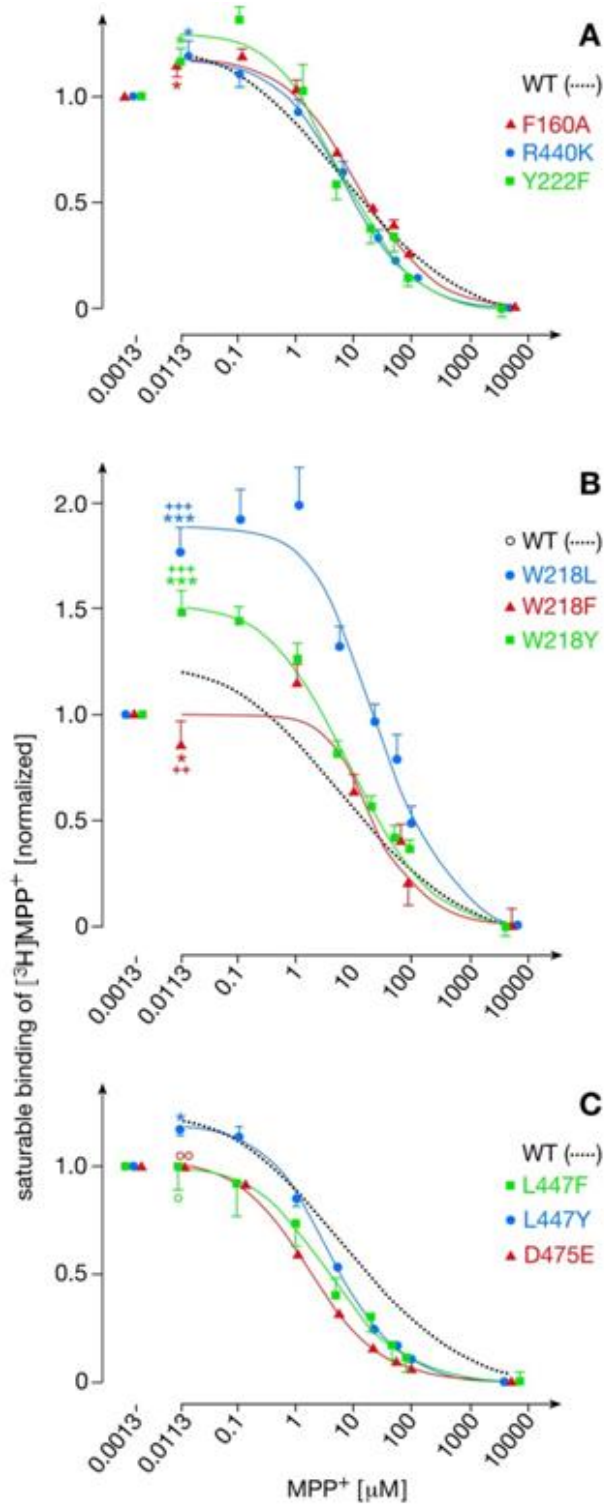


Figure 8. Effects of mutations within the inner part of the modeled outward-open cleft of rOCT1 on saturable binding of MPP $^+$ measured at 0°C.

Concentration dependence of binding of MPP^+ to *rOCT1* mutants stably expressed in HEK293 cells was measured. Mean values \pm S.E.M of 12 measurements from 3 independent experiments are indicated. The curves were obtained by fitting the Hill equation to the data excluding the values measured at 1.25 nM MPP^+ . Student's *t*-test: * $P < 0.05$, ** $P < 0.01$, *** $P < 0.001$, difference between [3H] MPP^+ binding measured at 11.25 nM MPP^+ versus 1.25 nM MPP^+ ; o $P < 0.05$, oo $P < 0.01$, difference of [3H] MPP^+ binding to *rOCT1* wild-type measured at 11.25 nM MPP^+ ; ANOVA, Newman-Keuls tests: ++ $P < 0.01$, +++ $P < 0.001$, difference of [3H] MPP^+ binding to *rOCT1* wild-type measured at 11.25 nM MPP^+ .

rOCT1 Mutants	Binding of MPP K _D [μ M]
Wild-type	4.87 \pm 1.0
F160A	9.07 \pm 1.89**
W218F	14.1 \pm 1.42***, $\Delta\Delta$
W218Y	5.93 \pm 1.26 $\Delta\Delta$
W218L	15.8 \pm 0.35***
Y222F	3.97 \pm 1.17
R440K	5.63 \pm 0.70
L447F	3.33 \pm 0.65
L447Y	3.83 \pm 0.59
D475E	1.50 \pm 0.45**, Δ
K215R	60.2 \pm 9.3***

Table 1. Binding of [3H] MPP^+ to HEK293 cells stably transfected with *rOCT1* wild-type or *rOCT1* mutants was measured at 0°C. Binding of 1.25nM [3H] MPP^+ was measured without the addition of non-radioactive MPP^+ , in the presence of 8 concentrations of non-radioactive MPP^+ between 10 nM and 100 μ M, and after the addition of 5 mM non-radioactive MPP^+ . Saturable [3H] MPP^+ binding was determined by subtracting non-specific binding at 5 mM MPP^+ . Three independent binding experiments with 4 measurements per ligand concentration were performed. K_D values were determined by fitting the Hill equation to individual experiments. Because in most experiments binding measured at the lowest employed MPP^+ concentration (1.25nM) was lower compared to binding at 11.25 nM MPP^+ , MPP^+ binding at 1.25 nM MPP^+ was excluded from the fit. Mean K_D values \pm S.D. of 3 measurements are shown. ANOVA, Newman-Keuls tests: * $P < 0.05$, ** $P < 0.01$, * $P < 0.001$ difference to *rOCT1* wild-type; Student's *t*-test: Δ $P < 0.05$, $\Delta\Delta$ $P < 0.01$ difference to K_m for MPP^+ (H. Koepsell, V. Gorboulev, U. Roth, unpublished data).**

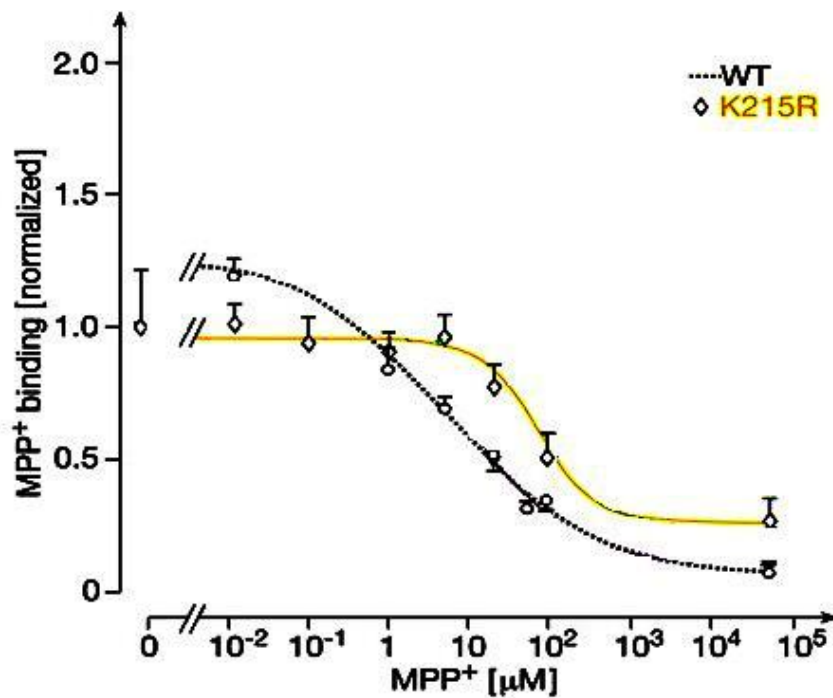


Figure 9. Binding of [³H]MPP⁺ to the non-transporting rOCT1 mutant, K215R.

Concentration dependence of binding of MPP⁺ to rOCT1 mutants stably expressed in HEK293 cells was measured. Mean values ± S.E.M of 12 measurements from 3 independent experiments are indicated. The curves were obtained by fitting the Hill equation to the data excluding the values measured at 1.25 nM MPP⁺.

4.2 [^{14}C]TEA $^+$ binding

4.2.1 [^{14}C]TEA $^+$ binding to rOCT1 wild-type expressed in HEK293 cells

The binding assay for [^{14}C]TEA $^+$ binding was done in the same manner as for MPP $^+$ binding. The range of 8 different concentrations of TEA $^+$ used in the experiments consisted of the basic concentration of 2 μM (only radioactive TEA $^+$) to a final concentration of 10 mM made by adding increasing amount of non-radioactive TEA $^+$.

While optimizing the binding of [^{14}C]TEA $^+$ to rOCT1 wild-type and its mutants, we encountered a surprising result. The binding of this substrate to the rOCT1 wild-type expressing cells was very low and not significantly different from that of HEK293 cells transfected with the empty vector (Fig.10). We hypothesized that perhaps the frozen state of the transporter rendered the binding site of TEA $^+$ in rOCT1 wild-type inaccessible to TEA $^+$.

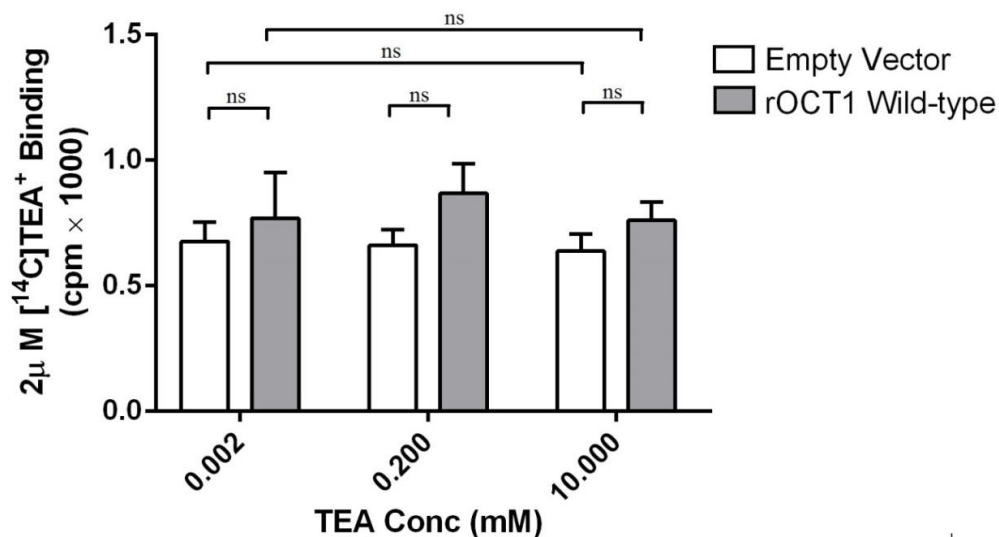


Figure 10. [^{14}C]TEA $^+$ binding to expression-vector and rOCT1 wild-type expressed in HEK293 cells.

Optimization of the analysis of [^{14}C]TEA $^+$ binding to pelleted HEK293 cells expressing empty vector and rOCT1 wild-type. Stably transfected HEK293 cells were incubated for 5 min at 0°C with 2 μM [^{12}C]TEA $^+$ in the presence of different concentrations of non-radioactive TEA $^+$ making the final concentration 0.2 mM and 10 mM. The cells were pelleted and radioactivity in the pellet was analyzed after a rapid wash of the surface of the pellet to remove remaining supernatant (1 second wash). rOCT1 wild-type expressing HEK293 cells didn't show any binding similar to empty vector transfected cells. Mean values \pm S.D of 12 measurements from 3 independent experiments are shown. ** $P < 0.01$, *** $P < 0.001$ significance of difference determined by ANOVA with posthoc Newman-Keuls tests.

4.2.2 [¹⁴C]TEA⁺ binding to rOCT1 mutants expressed in HEK293 cells

Unlike rOCT1 wild-type, the mutants expressed in HEK293 cells displayed varied results for [¹⁴C]TEA⁺ binding (Table 2, Fig.11). Concentration dependent replacement of 2 μM [¹⁴C]TEA⁺ was observed after addition of higher TEA⁺ concentrations only in some of the mutants. Fitting the Hill equation to the concentration-dependent replacement curve starting at the TEA⁺ concentration of 2 μM, very high K_D values were obtained. These values were more than five-fold higher than the apparent K_m value of TEA⁺ transport measured in HEK293 cells at 37°C (H. Koepsell, V. Gorboulev, U. Roth, unpublished data). When Asp475 was replaced by glutamate, a very high K_D value of 652.5 μM was obtained. This result is in sharp contrast to that of uptake assays with this mutant where the K_m is decreased. It is possible that this mutant, due to different conformations in a frozen state allows a very strong binding leading to a high K_D value but at 37°C favors the transport of substrate with a high affinity resulting in a decreased K_m. Replacement of tryptophan at position 218 by either phenylalanine (W218F), or leucine (W218L) or tyrosine (W218Y) did not result in any binding just like the rOCT1 wild-type. After replacing Phe160 with alanine, Tyr222 with phenylalanine and Arg440 with lysine again very high K_D values were observed. If the Leu447 was replaced by tyrosine, this mutant (L447Y) showed no binding of [¹⁴C]TEA⁺ but an extremely low-affinity binding was detected when the replacement was done by phenylalanine (L447F). The only explanation we could give was a different accessibility of the substrate TEA⁺ to the binding site at 0°C in the outward open conformation due to the mutations.

rOCT1 Mutants	Binding of [¹⁴ C]TEA ⁺ K _D (μM)
Wild Type	No binding
D475E	652.5 ± 14.8 ****
F160A	314.7 ± 49.2***
L447F	1208.13 ± 222.8**
L447Y	No binding
R440K	174.1 ± 32.6**
W218F	No binding
W218L	No binding
W218Y	No binding
Y222F	242.1 ± 56**
K215R	No binding

Table 2. Binding of [¹⁴C]TEA⁺ to HEK293 cells stably transfected with rOCT1 wild-type or rOCT1 mutants was measured at 0°C.

Binding of 2 μM [¹⁴C]TEA⁺ was measured in the presence of 8 concentrations of non-radioactive TEA⁺ between 2 μM and 5 mM, and after the addition of 10 mM non-radioactive TEA⁺. Saturable [¹⁴C]TEA⁺ binding was determined by subtracting non-specific binding at 10 mM MPP⁺. Three independent binding experiments with 4 measurements per cation concentration were performed. K_D values were determined by fitting the Hill equation to individual experiments. Mean K_D values ± S.D. of 3 measurements are shown. Student's t-test: **** P<0.0001, *** P<0.001, ** P<0.01 difference to K_m for TEA⁺ (H. Koepsell, V. Gorboulev, U. Roth, unpublished data).

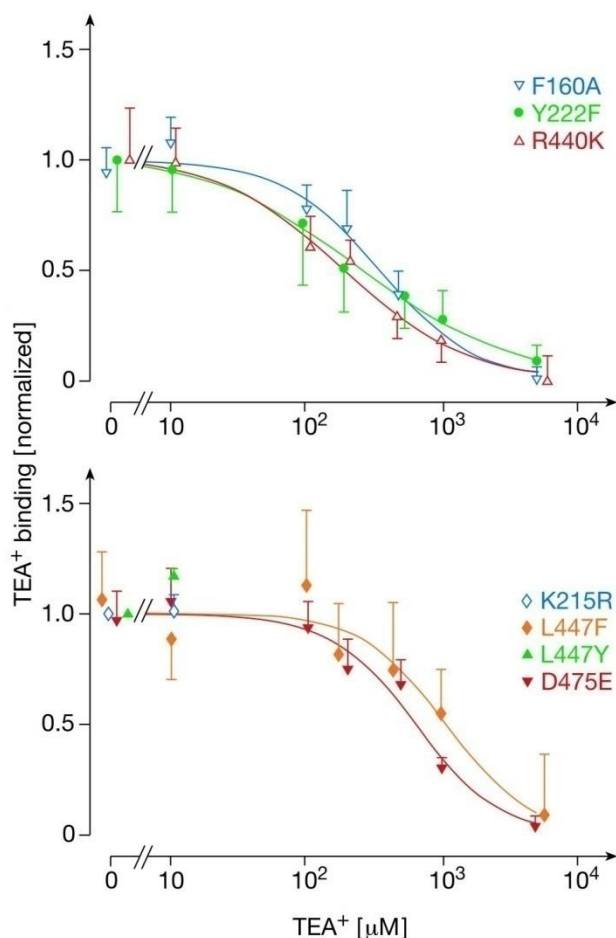


Figure 11. Effects of mutations within the inner part of the modeled outward-open cleft of rOCT1 on saturable binding of $[^{14}\text{C}]\text{TEA}^+$ measured at 0°C .

Concentration dependence of binding of TEA^+ to rOCT1 mutants stably expressed in HEK293 cells was measured. Mean values \pm S.E.M of 12 measurements from 3 independent experiments are indicated. The curves were obtained by fitting the Hill equation to the data.

4.2.3 $[^{14}\text{C}]\text{TEA}^+$ binding to rOCT1 wild-type measured in K^+ -phosphate buffer

The buffer present in the environment of the system may affect the conformation of the proteins and thus we tried changing the conformation of our transporter by changing the buffer in order to check $[^{14}\text{C}]\text{TEA}^+$ binding to rOCT1 wild-type. All the experiments described in this chapter were performed throughout (including the cell culture) in K^+ -phosphate buffer. The binding of 1.25 nM $[^3\text{H}]\text{MPP}^+$ was checked in the presence of a range of non-radioactive MPP^+ (from 1.25 nM till 5 mM MPP^+ as the final concentration) as a control. Concentration dependent replacement of

1.25 nM [^3H]MPP $^+$ was observed after addition of higher MPP $^+$ concentrations. Fitting the Hill equation to the replacement curve starting at the MPP $^+$ concentration of 11.25 nM, a K_D value of $5.9 \pm 1.7 \mu\text{M}$ was obtained which was not significantly different from the apparent K_D value for binding of MPP $^+$ measured in Na $^+$ -phosphate buffer (Fig. 12). However, we could not see any replaceable binding of $2\mu\text{M}$ [^{14}C]TEA $^+$ in the presence of different concentrations of non-radioactive TEA $^+$. The results indicate that the conformation change was not significant enough to affect the binding of the substrates to the transporter.

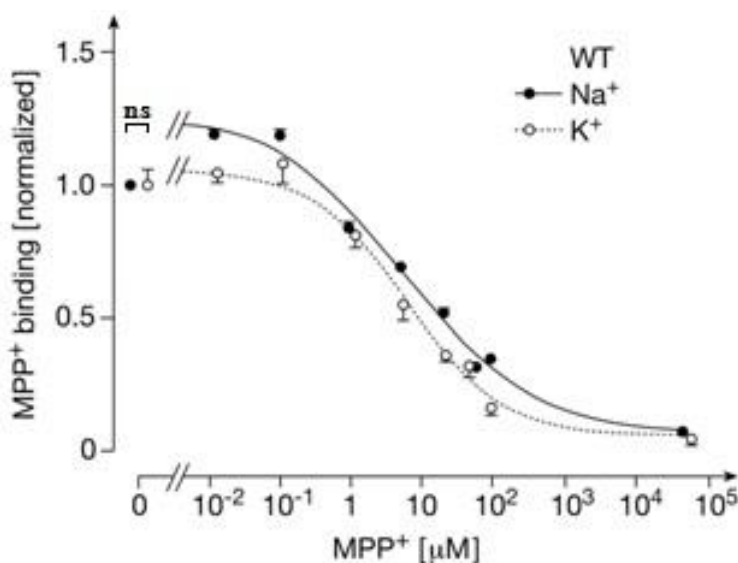


Figure 12. [^3H]MPP $^+$ binding to rOCT1 wild-type measured in K $^+$ -phosphate buffer
Concentration dependence of binding of MPP $^+$ to rOCT1 wild-type stably expressed in HEK293 cells was measured in the presence of K $^+$ -phosphate buffer at 0°C. Mean values \pm S.E.M of 12 measurements from 3 independent experiments are indicated. The curves were obtained by fitting the Hill equation to the data excluding the values measured at 1.25 nM MPP $^+$. (Student's *t*-test: * $P < 0.05$, ** $P < 0.01$, *** $P < 0.001$, Difference between [^3H]MPP $^+$ binding measured in PBS and K $^+$ -phosphate buffer.)

4.3. Substrate binding inhibition studies at 0°C

Previous studies have pointed out towards the possibility of overlapping binding sites for MPP $^+$ and TEA $^+$. So, we checked the inhibition of [^3H]MPP $^+$ binding in the presence of non-radioactive TEA $^+$ at 0°C and *vice versa*.

4.3.1 [^3H]MPP $^+$ binding to rOCT1 wild-type in the presence of non-radioactive TEA $^+$ at 0°C

The inhibition of 1.25 nM [^3H]MPP $^+$ binding at 0°C to rOCT1 Wild-type was done using different concentrations of non-radioactive TEA $^+$ ranging from 0.1 μM to 1 mM (including the zero-point). The experiments were performed in the same manner as the earlier optimized binding assay (in PBS). HEK293 cells stably transfected with rOCT1 were incubated for 5 min at 0°C with 1.25 nM [^3H]MPP $^+$. The cells were pelleted and radioactivity in the pellet was analyzed after a rapid 1s wash of the surface of the pellet to remove remaining supernatant. The result showed a successful replacement of [^3H]MPP $^+$ by TEA $^+$ with an IC $_{50}$ value of about 58.4 ± 7.7 μM (Fig. 13). Interestingly, the addition of TEA $^+$ in concentrations from 0.1 μM to 10 μM led to continuous increase in MPP $^+$ binding that was at 10 μM TEA $^+$ almost 100% (as compared to zero-point). This increase can be attributed to an allosteric interaction between MPP $^+$ and TEA $^+$ binding sites. The data also confirms the existence of overlapping binding sites for the substrates MPP $^+$ and TEA $^+$ and also indicate that in the frozen state, a pre-binding of MPP $^+$ to the transporter somehow allowed access of TEA $^+$ due to which it could replace MPP $^+$.

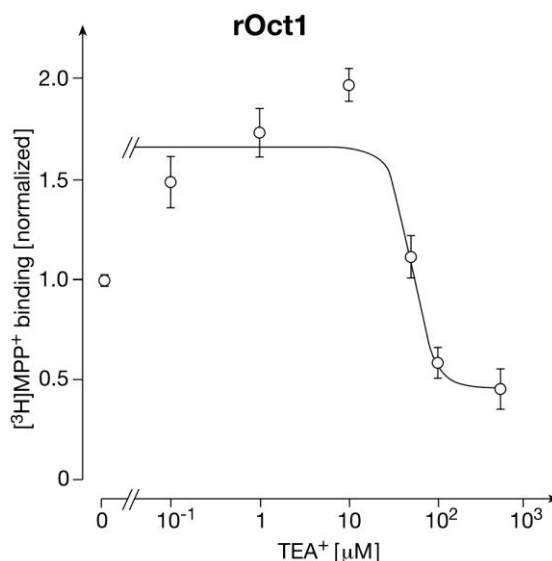


Figure 13. Replacement of 1.25 nM [^3H]MPP $^+$ by non-radioactive TEA $^+$

Replacement was done in the presence of 8 concentrations of non-radioactive TEA $^+$ ranging from 0.1 μM to 10 mM (including the zero-point). Mean values \pm S.E.M of 12 measurements from 3 independent experiments are indicated. The curve was obtained by fitting the Hill equation to the data.

4.3.2 [^{14}C]TEA $^+$ binding to rOCT1 wild-type and mutant (D475E) in the presence of non-radioactive MPP $^+$

To investigate whether the TEA $^+$ binding site in the outward open cleft becomes accessible after MPP $^+$ has bound we measured replaceable binding of 2 mM [^{14}C]TEA $^+$ binding to rOCT1 wild-type and rOCT1 (D475E) in the presence of 8 different concentrations of non-radioactive MPP $^+$ ranging from 0.1 μM to 2 mM (including the zero-point). [^{14}C]TEA $^+$ showed no binding in rOCT1 wild-type as before (*data not shown*). However, we did see a successful inhibition/replacement of [^{14}C]TEA $^+$ by non-radioactive MPP $^+$ in rOCT1 (D475E) mutant (*Fig. 14*), the same mutant that showed a binding of TEA $^+$ with a very low affinity (*Fig. 11, Table 2*). This result is consistent with the fact that MPP $^+$ has a high affinity of binding to rOCT1 wild-type as compared to TEA $^+$. The calculated IC $_{50}$ value for inhibition of 2 mM [^{14}C]TEA $^+$ binding by non-radioactive MPP $^+$ in rOCT1 (D475E) was $6.5 \pm 1.2 \mu\text{M}$. The data re-affirmed the overlapping nature of the binding sites for MPP $^+$ and TEA $^+$.

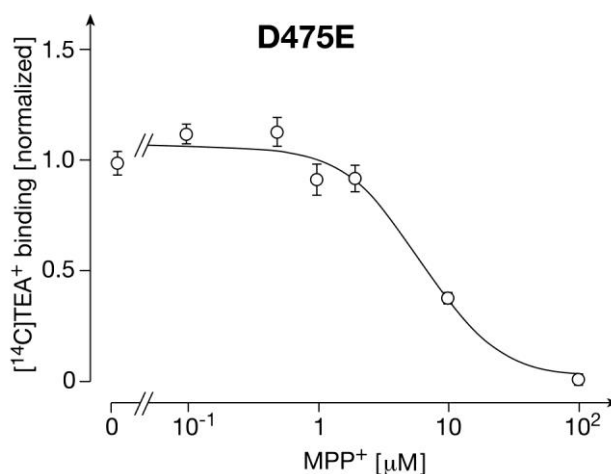


Figure 14. Replacement of 1.25 nM [^3H]MPP $^+$ by non-radioactive TEA $^+$
Replacement was done in the presence of 8 concentrations of non-radioactive MPP $^+$ ranging from 0.1 μM to 2 mM (including the zero-point). Mean values \pm S.E.M of 12 measurements from 3 independent experiments are indicated. The curve was obtained by fitting the Hill equation to the data.

5. Discussion

In the present study, an attempt was made to develop a method for measuring the binding (K_D) of substrates MPP^+ and TEA^+ to rOCT1 at 0°C . When we measure K_m , as has been done using the uptake assays at 37°C , we allow not only the ligand to bind the transporter but also to undergo all the changes that are a likely result of that binding, including the conformational changes of the transporter and an inward journey of the ligand. Therefore, the K_m that is measured is a complex constant based on a number of rate constants which becomes even more complex with increasing number of steps involved in translocation (*Fig.15*). Although, it is a good tool to measure the affinity of the transporter for the ligand as well as the rate and efficiency of transportation, it is not very helpful in defining exactly which step of the transport is rate-limiting. Also, we cannot attribute the changes that are observed in the K_m value after inserting point mutations in the transporter only to the outward-binding conformation of the transporter. So, we tried to make measurements at a temperature which did not allow the transporter to make any conformational change and allowed us to safely predict that any interaction with the ligand took place in the outward-open conformation. Any effects in the K_D value (*Fig.15*) due to point mutations that showed up were when the transporter was in the outward-open form.

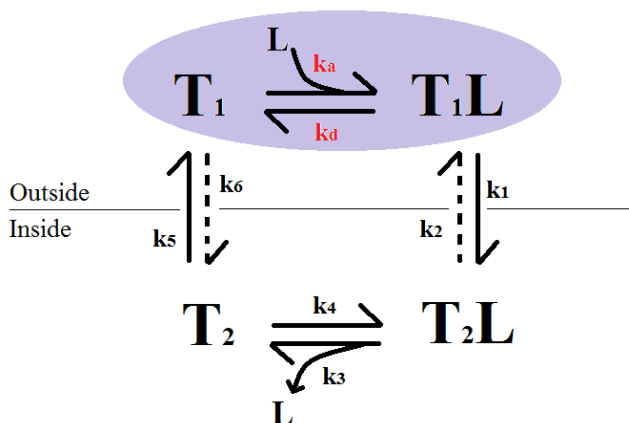


Figure 15. A simple model depicting the rate constants that are presumably involved at various steps of transport by rOCT1.

T_1 and T_2 denote the outward and the inward open conformations of the transporter respectively and L is the ligand. T_1L and T_2L are the complexes of ligand bound to the transporter. Equilibrium dissociation constants for ligand binding are $K_D = k_d/k_a$ and k_3/k_4 whereas rate constants for transporter reorientation are k_1 , k_2 , k_5 and k_6 .

When [^3H]MPP $^+$ binding was measured to stably transfected HEK293 cells at 0°C, a K_D value of $4.87 \pm 1.0 \mu\text{M}$ was obtained for rOCT1 wild-type which was not significantly different from the K_m value measured through uptake assays at 37°C that was $4.7 \pm 0.8 \mu\text{M}$ (Table 3). Also after addition of 10 nM non-radioactive MPP $^+$, an initial increase of about 20% in bound MPP $^+$ was observed (Fig. 7). This points towards the existence of more than one binding site (both high and low-affinity) that have an allosteric interaction, i.e., substrate binding to the high-affinity binding site brings about an allosteric change in the low affinity binding sites allowing them to bind the substrate more quickly. Some conclusions that we can draw from this observation are:

- Both the high as well as the low affinity binding sites are available in the outward-open cleft of rOCT1,
- the K_m for binding of MPP $^+$ is dependent on the structure of the outward-open conformation
- There is no difference in the structure of the binding site at 37°C and 0°C.

Mutations at position Trp218, Phe160 and Asp475 resulted in a change in the K_D value (Table 3). When compared with the K_m values obtained through uptake assays at 37°C, it was observed that replacing Trp218 with Leu (W218L) resulted in a decrease in affinity in terms of both K_m and K_D . However, varying results were observed in the mutants W218F and W218Y. After replacement with phenylalanine at this position the K_D increased three-fold but the K_m didn't change. On the other hand, when we replaced Trp218 with tyrosine the K_D remained unchanged but the K_m decreased significantly (about six-fold). The mutants W218L and W218Y also showed an increase similar to rOCT1 wild-type on addition of 10 nM non-radioactive MPP $^+$ (Fig. 8). This increase in [^3H]MPP $^+$ binding was 86% in case of W218L and 49% in W218Y as compared to the 20% increase in rOCT1 wild-type. At variance, in the third mutant of this category, W218F, this effect was totally absent. Apart from an indication of the fact that Trp218 is involved in the allosteric interactions between the high-affinity and the low-affinity binding sites, these results also point out the existence of a more complex role that this position has in the binding of MPP $^+$ to the outward-open cleft of rOCT1. The data indicate that the affinity for transport is not dependent on the extracellular MPP $^+$ -binding to low affinity sites.

The presence of more than one binding sites has also been demonstrated by checking [^3H]MPP $^+$ binding to purified rOCT1 reconstituted into nanodiscs (T. Keller, V. Gorboulev, T. Mueller, V.

Doetsch, V. Gorboulev, G. Bernhard, H. Koepsell, unpublished data). The lipid bilayer in these nanodiscs was made up of either di-myristoyl phosphatidylcholine (DMPG) or palmitoyloleoyl phosphatidylcholine (POPC) and was framed by membrane scaffold protein 1 (MSP1). Cell-free expressed rOCT1 was co-translationally incorporated into these nanodiscs and binding of MPP^+ was measured (dissociation constant, K_D and maximal binding, B_{max}) using a filter assay. It was detected that 2 MPP^+ molecules bound per rOCT1 monomer and one K_D value of about 30 μM was calculated with nanodiscs that were formed from DMPG. As for the nanodiscs formed from POPC, three MPP^+ molecules were observed to bind per monomer of rOCT1 wild-type. For two of these molecules a common low affinity of about 36 μM was detected whereas for the third MPP^+ molecule a high affinity K_D value of 0.24 μM was obtained. When MPP^+ -transport was checked in proteoliposomes containing rOCT1 wild-type, only a single K_m value of about 19 μM was obtained (*Keller T et. al., 2008*). The data in nanodiscs thus indicates the presence of two transport-related low-affinity binding sites plus a high-affinity binding site. However, these nanodisc experiments could not distinguish between binding of MPP^+ to outward-open and inward-open cleft of rOCT1. This is because both the states are mutually exclusive in this system. Different lipid microenvironment, phosphorylation of rOCT1 in cells and interaction with cellular proteins are some of the factors that can lead to difference in results obtained through nanodisc experiments and through binding assays done in intact cells. Two individual MPP^+ -binding sites with low and high affinities were also titrated using voltage clamp fluorometry on a fluorescent labeled rOCT1 variant (*Gorbunov et. al., 2008*).

Another mutant that showed a similar result in case of both the present binding assay at 0°C and uptake assay at 37°C was F160A. In both the cases the affinity decreased about 2 fold (*Table 3*). This leads us to the conclusion that Phe160 is not only directly involved in MPP^+ binding to rOCT1 but also directly involved in transport as well. When Asp475 was replaced with glutamate (D475E), the results were again different for both assays. The K_m value measured at 37°C was not altered but the K_D value measured at 0°C decreased three-fold thus giving us an indication that Asp475 is important for binding of MPP^+ to rOCT1 but is probably not directly involved in its translocation to the other side (*Table 3*). The above mentioned nanodisc experiments conducted with the mutant rOCT1-D475E also showed a 25% decrease in the K_D value for low-affinity site (*T. Keller, V. Gorboulev, T. Mueller, V. Doetsch, V. Gorboulev, G.*

Bernhard, H. Koepsell, unpublished data). The parallels drawn between the results of present study and that of the nanodisc studies on the positions Asp475 clearly indicate that this position is a part of at least one low-affinity binding site for MPP⁺ and the interaction at the outward side with MPP⁺ may or may not be through direct binding.

Both the K_D and K_m values remained unchanged after Tyr222 was replaced by phenylalanine (Y222F), Arg440 by lysine (R440K) and Leu447 by phenylalanine (L447F) or tyrosine (L447Y) ruling out the possibility of their direct involvement in binding of MPP⁺ (*Table 3*). Nanodisc experiments conducted on Leu447 mutants (L447F, L447Y) also showed that they did not reduce the number of MPP⁺ molecules bound per rOCT1 monomer indicating that Leu447 is not directly involved in MPP⁺-binding to the low-affinity binding site (*T. Keller, V. Gorboulev, T. Mueller, V. Doetsch, V. Gorboulev, G. Bernhard, H. Koepsell, unpublished data*).

Noteworthy was the result of binding of [³H]MPP⁺ to the non-transporting mutant K215R (which showed no uptake). We could measure some degree of low affinity MPP⁺ binding to this mutant supporting our belief that we measured binding and not transport in the present study.

The data suggest that the positions at which mutations affected the K_D value are involved in MPP⁺-binding to rOCT1 but whether this involvement is direct or through a change in substrate binding domain is still unclear.

rOCT1 Mutants	Binding of [³ H]MPP ⁺ K _D [μM]	Uptake of [³ H]MPP ⁺ K _m [μM]
Wild-type	4.87 ± 1.0	4.7 ± 0.8
D475E	1.5 ± 0.45 ^{**} , ^Δ	4.9 ± 2.0
F160A	9.07 ± 1.89 ^{**}	10.6 ± 0.9
L447F	3.33 ± 0.65	3.1 ± 0.7
L447Y	3.83 ± 0.59	5.6 ± 1.5
R440K	5.63 ± 0.70	4.2 ± 1.0
W218F	14.1 ± 1.42 ^{***} , ^{ΔΔ}	5.0 ± 1.8
W218L	15.8 ± 0.35 ^{***}	11.9 ± 1.8
W218Y	5.93 ± 1.26 ^{ΔΔ}	0.75 ± 0.09
Y222F	3.97 ± 1.17	5.0 ± 1.8
K215R	60.2 ± 9.3 ^{***}	No uptake

Table 3. Comparison of [³H]MPP⁺ binding and uptake by rOCT1 wild-type and its mutants expressed stably in HEK293 cells

Mean values ± S.D of 12 measurements from 3 independent experiments are shown. **P*<0.05, ***P*<0.01, ****P*<0.001 difference to WT; Student's *t*-test: ^Δ *P*<0.05, ^{ΔΔ} *P*<0.01 difference to *K_m* for MPP⁺ (H. Koepsell, V. Gorboulev, U. Roth, unpublished data).

Modeling of the outward-open conformation of rOCT1 was done by applying the en-bloc rearrangement mechanism of the two pseudosymmetric halves of the modeled inward-facing conformation of rOCT1 based upon the conformational change of LacY during transport (Abramson *J et. al.*, 2003; Gorbunov *D et. al.*, 2008). According to this model, in the outward-facing conformation, Phe160, Arg440 and Asp475 are located in the center of the transporter somewhat deeper into the outward-open cleft probably occupying a position critical for substrate binding (Fig.16A,B). Tyr222 is located at the bottom of the cleft closer to the cytosolic side indicating its role during the transport rather than initial binding of the substrate. If we view this model from the extracellular side (Fig.16B) we can observe a division of the binding cleft into three regions lined by Asp475, Trp218 and Phe160, by Asp475, Trp 218 and Leu447, and by Tyr222 and Arg440 thus confirming the results of the present study as well as the nanodisc experiments that have indicated the existence of more than one binding site (possibly three, 2 low-affinity binding sites and one high-affinity binding site) for MPP⁺. Docking of MPP⁺ molecules to the modeled outward-open cleft of rOCT1 suggests that MPP⁺ directly interacts

with Trp218 and Asp475 (*Fig.16*) and also explains the lack of interaction with Tyr222 and Leu447 as they seem to be located deeper inside the cleft probably having a role in ligand interaction either during transport or during the release of the substrate on the inside. The data of binding assays and nanodiscs experiments support the modeled outward-open conformation of rOCT1 and *vice versa*.

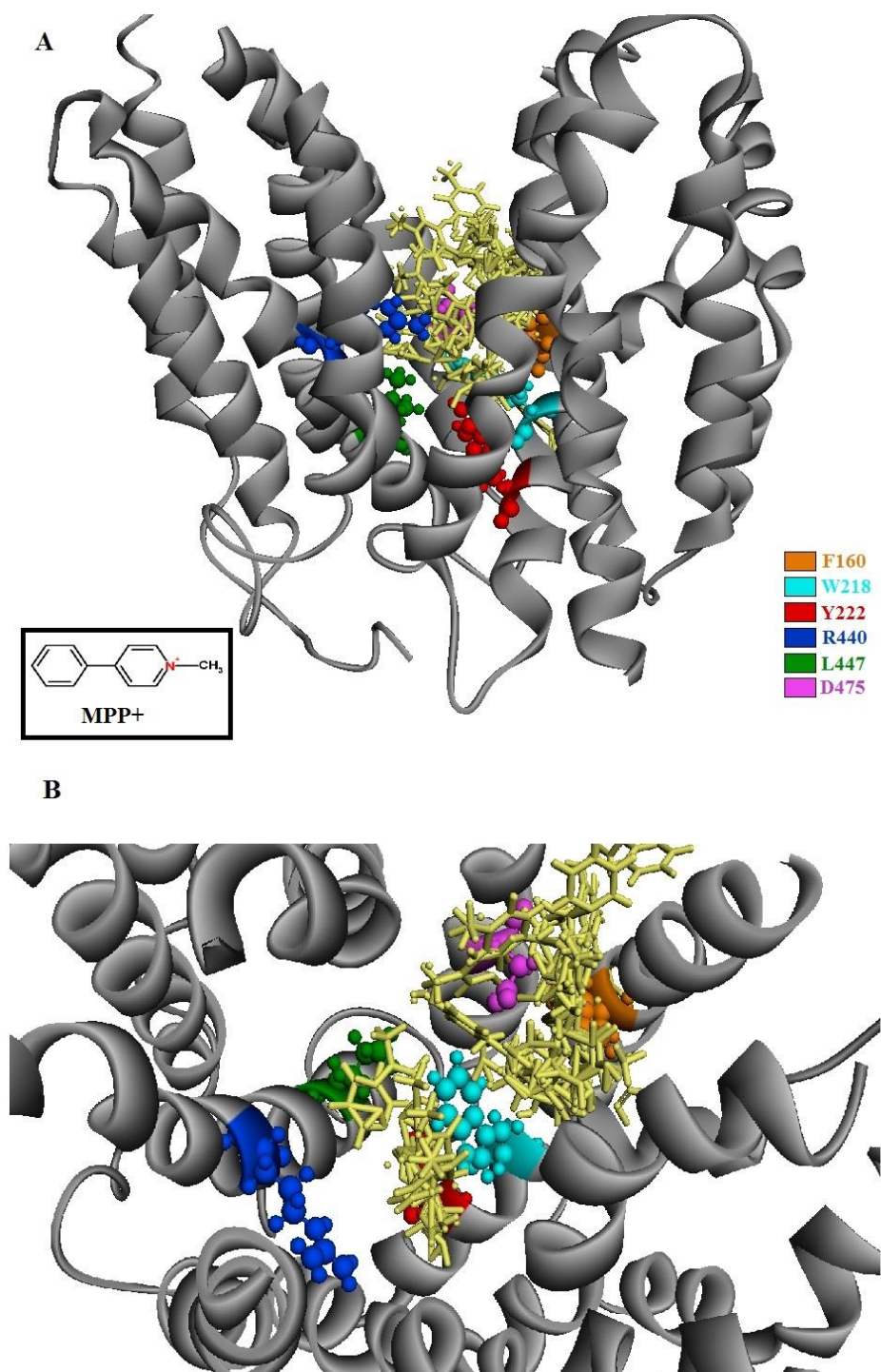


Figure 16. Structural model of rOCT1 in the outward-open conformation docked with MPP⁺ (in yellow) molecules showing the positions under study.

Modeling of the outward- and inward-open conformation was done using tertiary structures of LacY in the outward-open conformation. (A) Side-view and (B) View from outside of the outward open-conformation. (Courtesy: T. Mueller)

Interaction of rOCT1 with its other substrate, TEA⁺ at 0°C yielded surprising results. The rOCT1 wild-type did not show any binding of [¹⁴C]TEA⁺ although through uptake assay at 37°C a K_m of 67 ± 9.9 μM could be measured (*Fig.17, Table 4*). A possible explanation for this could be that in the frozen state the binding site for TEA⁺ was rendered inaccessible to it. Apart from wild-type, the binding site remained inaccessible when any change was made at position Trp218 (W218F, W218L and W218Y) as well. However, when compared with the uptake measurements, only the mutant W218L showed an absence of transport. In HEK293 cells stably transfected with rOCT1 (W218Y) the K_m for TEA⁺ was not changed but in rOCT1 (W218F) it was increased almost three-fold as compared to rOCT1 wild type. Leu447, when replaced with tyrosine (L447Y) also didn't show binding of [¹⁴C]TEA⁺ at 0°C. The rest of the mutants, namely D475E, F160A, L447F, R440K and Y222F showed very low affinity binding to TEA⁺ with a very high K_D value as compared to the corresponding K_m values (*Table4*).

The buffer present in the environment of the system may affect the conformation of the proteins (*Sydney O. Ugwu et. al., 2004*) and thus we tried changing the conformation of our transporter by changing the buffer in order to check [¹⁴C]TEA⁺ binding to rOCT1 wild-type. We could not see any binding of 2μM [¹⁴C]TEA⁺ in the presence of different concentrations of non-radioactive TEA⁺. The results indicate that the conformation change was not significant enough to affect the binding of the substrates to the transporter.

Both MPP⁺ and TEA⁺ belong to Type I OCs (<500 Da) and are strongly hydrophilic but are different structurally (*Schmitt BM et. al., 2005; Meijer DK et. al., 1990*). The binding of rOCT1 to structurally different cations is due to its polyspecificity which in turn can be attributed to transport related conformational changes induced by polyspecific cation binding. This polyspecific cation binding requires cation binding to several binding sites that interact with different ligand structures. Through uptake assays at 37°C, it has been shown that rOCT1 mediated transport of TEA⁺ is competitively inhibited by MPP⁺ and vice versa leading to the conclusion that MPP⁺ and TEA⁺ have overlapping binding sites. Following this idea, we tried the inhibition of [³H]MPP⁺ binding by non-radioactive TEA⁺ and *vice versa*. As expected, the binding of [³H]MPP⁺ to rOCT1 wild-type stably expressed in HEK293 cells could be replaced by TEA⁺ at 0°C with an IC₅₀ value of 58.4 ± 7.7 μM (*Fig. 11*). This was slightly higher than the IC₅₀ value observed for [³H]MPP⁺ uptake inhibition by TEA⁺ at 37°C (42 ± 7.1 μM). The result was

consistent with the overlapping nature of binding sites for MPP⁺ and TEA⁺. This result also suggests that the binding site for TEA⁺, inaccessible to it at 0°C when it interacted alone, somehow became accessible in the presence of [³H]MPP⁺, perhaps by a “pre-binding” of [³H]MPP⁺ molecules.

As for [¹⁴C]TEA⁺ binding inhibition at 0°C by non-radioactive MPP⁺, it was observed that it showed no binding in rOCT1 wild-type once again. However, when this was checked in the mutant rOCT1 (D475E) we could easily observe a smooth replacement of [¹⁴C]TEA⁺ by non-radioactive MPP⁺ (Fig. 12). This result is consistent with fact that MPP⁺ has a higher affinity for rOCT1 wild-type as compared to TEA⁺ and confirms the overlapping nature of the binding sites as well.

rOCT1 Mutants	Binding of [¹⁴ C]TEA ⁺ K _D [μM]	Uptake of [¹⁴ C]TEA ⁺ K _m [μM]
Wild-type	No binding	67 ± 9.9
D475E	652.5 ± 14.8****	19 ± 2.9
F160A	314.7 ± 49.2***	57 ± 8.3
L447F	1208.13 ± 222.8**	167 ± 23
L447Y	No binding	80 ± 6.1
R440K	174.1 ± 32.6**	32 ± 6
W218F	No binding	230 ± 28
W218L	No binding	No uptake
W218Y	No binding	61 ± 7.2
Y222F	242.1 ± 56**	55 ± 11

Table 4. Comparison of [¹⁴C]TEA⁺ binding and uptake by rOCT1 wild-type and its mutants expressed stably in HEK293 cells

Mean values ± S.D of 12 measurements from 3 independent experiments are shown. **P<0.01, ***P<0.001, ****P<0.0001 significance of difference determined by ANOVA with posthoc Newman-Keuls tests; Difference from the corresponding K_m value measured through uptake assays (H. Koepsell, V.Gorboulev and U. Roth, unpublished data)

In conclusion, we were able to measure K_D values during this study successfully for MPP⁺ binding by freezing our transporter rOCT1 at 0°C. The results supported the existence of more than one binding site for MPP⁺ and low and high affinity binding sites could be distinguished.

Cooperativity in binding of MPP^+ to these sites was also confirmed using some mutants. We were also able to confirm the overlapping nature of the binding sites for the substrates MPP^+ and TEA^+ . It was also possible to identify the amino acids in the binding site that interact with MPP^+ in the outward open conformation, namely Phe160, Trp218 and Asp475. The results obtained for TEA^+ binding were more complex as we did not see any binding of TEA^+ to rOCT1 wild-type. The amino acids which altered TEA^+ binding in the outward open conformation were Asp475, Phe160, Leu447, Arg440 and Tyr222.

6. Summary

The present study was conducted on the rOCT1, a member of SLC22 family. Structurally, it consists of 12 membrane spanning α -helices with both N- and C-termini intracellular. Studies done so far, through tracer uptake and inhibition, reconstitution of rOCT1 in nanodiscs and proteoliposomes and voltage-clamp fluorometry, have identified the main amino acids in the cleft of rOCT1 that interact in a critical manner with the substrates/inhibitors either directly or indirectly. Homology modeling studies have also supported these observations. In the present study we aimed at measuring the binding of substrates MPP⁺ and TEA⁺ to rOCT1 at 0°C in order to establish the amino acids in the cleft region that interact with the substrate when the transporter is frozen in the outward-open conformation. Previously identified crucial amino acids (Asp475, Phe160, Leu447, Arg440, Trp218 and Tyr222) were selected for the study. rOCT1 wild-type and its mutants were stably expressed in HEK293 cells and these cells were used for the binding measurements with the radioactive substrate (MPP⁺ or TEA⁺) at 0°C in Mg-Ca-PBS buffer as described in “Materials and Methods” section in detail. rOCT1 wild-type revealed for MPP⁺-binding a K_D which was not significantly different from the corresponding K_m value. Also, after addition of 10 nM non-radioactive MPP⁺, an initial increase of about 20% in bound MPP⁺ was observed. The results indicate that the K_m for transport is dependent on the binding of MPP⁺ to the outward-open conformation and hints at the possibility of allosteric interaction between the binding sites. Mutations at position Trp218, Phe160 and Asp475 resulted in a change in the K_D value. Trp218 mutations also showed an allosteric increase similar to the rOCT1 wild-type. This study suggests that these amino acids are located at a critical position in the outward-open conformation for MPP⁺ transport. TEA⁺-binding could not be observed in rOCT1 wild-type, indicating that the binding site is perhaps inaccessible for TEA⁺ in frozen outward-open state. The mutants D475E, F160A, L447F, R440K and Y222F showed a very low affinity binding with a very high K_D value as compared to the corresponding K_m values indicating that the transporter might have different affinities for extra-cellular binding alone and for the complete transport process especially if temperature is the limiting factor. Substrate inhibition studies done using both MPP⁺ and TEA⁺ have confirmed the existence of overlapping binding sites for these two ligands. This study has confirmed the direct interaction of Trp218, Phe160, Asp475 with MPP⁺ and Phe160, Asp475, Leu447, Arg440 and Tyr222 with TEA⁺ in the outward-open conformation.

7. Zusammenfassung

In der vorgelegten Arbeit werden Untersuchungen am organischen Transporter rOCT1, einem Mitglied der *SLC22* Familie, berichtet. Frühere Untersuchungen beinhalteten Transportmessungen mit radioaktiven Substanzen und Hemmstoffen, Transport- und Bindungsmessungen nach Rekonstitution in Nanodisken und Proteoliposomen und Voltage-Clamp-Fluorimetrie-Analysen an rOCT1 und rOCT1 Mutanten. Sie führten zur Identifizierung wichtiger Aminosäuren im Bindungsspalt von rOCT1, welche für die Interaktion mit Substraten oder Hemmstoffen wichtig sind. Homologiemodelle wurden zur Interpretation der Ergebnisse herangezogen. In der vorgelegten Arbeit haben wir die Bindung der Substrate MPP^+ und TEA^+ an rOCT1 bei 0°C gemessen um herauszufinden welche Aminosäuren in der Spaltregion von rOCT1 mit diesen Substraten interagieren, wenn der Transporter in der nach außen offenen Konformation „eingefroren“ ist. Für die Untersuchungen wurden Aminosäuren ausgewählt, deren Relevanz für den Transport von MPP^+ und TEA^+ in früheren Untersuchungen erkannt worden war. Es handelt sich um die Aminosäuren Asp475, Phe160, Leu447, Arg440, Trp218 und Tyr222. rOCT1 Wildtyp und rOCT1 Mutanten wurden stabil in HEK293 Zellen exprimiert. Mit diesen Zellen wurden bei 0°C Bindungsmessungen mit radioaktiv markiertem MPP^+ und TEA^+ unter Verwendung eines Magnesium und Calcium erhaltenen Puffers. Für die MPP^+ -Bindung an den rOCT1 Wildtyp ergab sich eine μmolare Dissoziationskonstante (K_D), die keinen signifikanten Unterschied zum früher gemessenen K_m Wert aufweist. Dieses Ergebnis zeigt, dass der K_m von der MPP^+ -Bindung an die nach außen offene Konformation abhängig ist. Bei der Zugabe von 10 nM nicht-radioaktivem MPP^+ war beim rOCT1 Wildtyp die Bindung von radioaktiv markiertem MPP^+ um 20% erhöht. Dies deutet auf einen allosterischen Effekt einer hochaffinen MPP^+ Bindungsstelle auf die direkt am Transport beteiligte μmolare Bindungsstelle hin. Mutationen der Aminosäuren Trp218, Phe160 und Asp475 führten zu Änderungen des K_D Wertes für die MPP^+ Bindung. Für die Mutanten von Trp218 wurde ein ähnlicher allosterischer MPP^+ Effekt wie beim rOCT1 Wildtyp beobachtet. Die Untersuchungen weisen darauf hin, dass diese drei Aminosäuren in kritischen Positionen für die MPP^+ -Bindung von außen befinden. Bei 0°C konnte beim rOCT1 Wildtyp keine TEA^+ -Bindung nachgewiesen werden. Dies legt den Schluss nahe, dass die TEA^+ -Bindungsstelle in der „eingefrorenen“ nach außen gerichteten Konformation unzugänglich ist. In Gegensatz dazu zeigen die Mutanten D475E, F160A, L447F, R440K und Y222F eine sehr niederaffine TEA^+ -Bindung mit hohen K_D Werten, die sich stark

von den entsprechenden K_m Werten unterscheiden. Durch Experimente, bei denen die Bindung von MPP^+ durch TEA^+ bzw. die Bindung von TEA^+ durch MPP^+ gehemmt wurde, wurde die Hypothese bestätigt, dass sich die Bindungsstellen für MPP^+ und TEA^+ überlappen. Unsere Untersuchungen deuten darauf hin, dass in der nach außen gerichteten Konformation von rOCT1 Trp218, Phe160 und Asp475 direkt mit MPP^+ und Phe160, Asp475, Leu447, Arg440 und Tyr222 direkt mit TEA^+ interagieren.

8. List of abbreviations

A, Ala	Alanine
ABC	ATP-binding cassette
ANOVA	Analysis of variance
ATP	Adenosine triphosphate
BCRP	Breast cancer resistance protein
BSA	Bovine serum albumin
C, Cys	Cysteine
CNS	Central nervous system
cpm	counts per minute
D, Asp	Aspartate
DMEM	Dulbecco's modified Eagle's medium
DMPG	Di-myristoyl phosphatidylcholine
DNA	Deoxyribonucleic acid
DPM	Disintegrations per minute
E, Glu	Glutamate
EMT	Extra-neuronal monoamines transporter
F, Phe	Phenylalanine
FCS	Fetal calf serum
Fuc P	Fucose P transporter
G418	Geneticin
HEK293	Human embryonic kidney cells
hOCT1	human Organic cation transporter
IC50	Half maximum inhibitory concentration
K, Lys	Lysine
K _D	Dissociation constant
K _m	Michaelis-Menten constant
L, Leu	Leucine
Lac Y	Lactose permease
M, Met	Methionine

MDR	Multi-drug resistance protein
MFS	Major facilitator superfamily
MPP ⁺	1-methyl-4-phenyl-pyridinium
MRP	Multi-drug resistance associated protein
MSPI	Membrane scaffold protein I
ns	not significant
OAT	Organic anion transporter
OC	Organic cation
OCT	Organic cation transporter
OCTN	Organic cation/zwitterions transporter
PBS	Phosphate buffer saline
PCR	Polymerase chain reaction
POPC	Palmitoyl oleyl phosphatidylcholine
Q, Gln	Glutamine
R, Arg	Arginine
RNA	Ribonucleic acid
rOCT1	rat Organic cation transporter 1
rpm	Rotations per minute
S.D.	Standard deviation
SDS	Sodium dodecyl sulphate
S.E.M.	Standard error mean
SLC	Solute carrier
T, Thr	Threonine
TBuA ⁺	Tetra butyl ammonium
TEA ⁺	Tetra ethyl ammonium
TMD	Transmembrane domain
TMH	Transmembrane helix
V _{max}	Maximum velocity of transport
W, Trp	Tryptophan
WT	Wild-type
Y, Tyr	Tyrosine

9. References

Abel S, Nichols DJ, Brearley CJ and Eve MD. 2000. Effect of cimetidine and ranitidine on pharmacokinetics and pharmacodynamics of a single dose of dofetilide. *Br J Clin Pharmacol.* 49(1):64-71.

Abramson J, Smirnova I, Kasho V, Verner G, Kaback HR and Iwata S. 2003. Structure and mechanism of the lactose permease of *Escherichia coli*. *Science.* 301(5633):610-5.

Andreev E, Brosseau N, Carmona E, Mes-Masson AM, Ramotar D. The human organic cation transporter OCT1 mediates high affinity uptake of the anticancer drug daunorubicin. 2016. *Sci Rep* ; 6:20508.

Anzai N, Kanai Y and Endou H. 2006. Organic anion transporter family: current knowledge. *J Pharmacol Sci.* 100(5):411-26.

Arndt P, Volk C, Gorboulev V, Budiman T, Popp C, Ulzheimer-Teuber I, Akhoundova A, Koppatz S, Bamberg E, Nagel G and Koepsell H. 2001. Interaction of cations, anions, and weak base quinine with rat renal cation transporter rOCT2 compared with rOCT1. *Am J Physiol Renal Physiol.* 281(3):F454-68.

Ayrton A and Morgan P. 2008. Role of transport proteins in drug discovery and development: a pharmaceutical perspective. *Xenobiotica.* 38(7-8):676-708.

Bachmakov I, Glaeser H, Fromm MF and König J. 2008. Interaction of oral antidiabetic drugs with hepatic uptake transporters: focus on organic anion transporting polypeptides and organic cation transporter 1. *Diabetes.* (6):1463-9.

Bachmakov I, Glaeser H, Endress B, Mörl F, König J and Fromm MF. 2009. Interaction of beta-blockers with the renal uptake transporter OCT2. *Diabetes Obes Metab.* (11):1080-3.

Barendt WM and Wright SH. 2002. The human organic cation transporter (hOCT2) recognizes the degree of substrate ionization. *J Biol Chem.* 277(25):22491-6.

- Budiman T, Bamberg E, Koepsell H and Nagel G. 2000. Mechanism of electrogenic cation transport by the cloned organic cation transporter 2 from rat. *J Biol Chem.* 275(38):29413-20.
- Burckhardt G and Burckhardt BC. 2011. In vitro and in vivo evidence of the importance of organic anion transporters (OATs) in drug therapy. *Handb Exp Pharmacol.* (201):29-104.
- Busch AE, Quester S, Ulzheimer JC, Waldegger S, Gorboulev V, Arndt P, Lang F and Koepsell H. 1996. Electrogenic properties and substrate specificity of the polyspecific rat cation transporter rOCT1. *J Biol Chem.* 271(51):32599-604.
- Busch AE, Karbach U, Miska D, Gorboulev V, Akhoundova A, Volk C, Arndt P, Ulzheimer JC, Sonders MS, Baumann C, Waldegger S, Lang F and Koepsell H. 1998. Human neurons express the polyspecific cation transporter hOCT2, which translocates monoamine neurotransmitters, amantadine, and memantine. *Mol Pharmacol.* 54(2):342-52.
- Ciarimboli G, Deuster D, Knief A, Sperling M, Holtkamp M, Edemir B, Pavenstädt H, Lanvers-Kaminsky C, am Zehnhoff-Dinnesen A, Schinkel AH, Koepsell H, Jürgens H and Schlatter E. 2010. Organic cation transporter 2 mediates cisplatin-induced oto- and nephrotoxicity and is a target for protective interventions. *Am J Pathol.* 176(3):1169-80.
- Dang S, Sun L, Huang Y, Lu F, Liu Y, Gong H, Wang J and Yan N. 2010. Structure of a fucose transporter in an outward-open conformation. *Nature.* 467(7316):734-8.
- Davidson MB and Peters AL. 1997. An overview of metformin in the treatment of type 2 diabetes mellitus. *Am J Med.* 102(1):99-110.
- Dresser MJ, Gray AT and Giacomini KM. 2000. Kinetic and selectivity differences between rodent, rabbit, and human organic cation transporters (OCT1). *J Pharmacol Exp Ther.* 292(3):1146-52.
- Dresser MJ, Leabman MK and Giacomini KM. 2001. Transporters involved in the elimination of drugs in the kidney: organic anion transporters and organic cation transporters. *J Pharm Sci.* 90(4):397-421.

- Egenberger B, Gorboulev V, Keller T, Gorbunov D, Gottlieb N, Geiger D, Mueller TD, Koepsell H. 2012. A Substrate Binding Hinge Domain Is Critical for Transport-related Structural Changes of Organic Cation Transporter 1. *J Biol Chem.* 287(37): 31561–31573
- Eisenhofer G. 2001. The role of neuronal and extraneuronal plasma membrane transporters in the inactivation of peripheral catecholamines. *Pharmacol Ther.* 91(1):35-62.
- Eraly SA, Hamilton BA and Nigam SK. 2003. Organic anion and cation transporters occur in pairs of similar and similarly expressed genes. *Biochem Biophys Res Commun.* 10;300(2):333-42.
- Eraly SA, Monte JC and Nigam SK. 2004. Novel slc22 transporter homologs in fly, worm, and human clarify the phylogeny of organic anion and cation transporters. *Physiol Genomics.* 17;18(1):12-24.
- Feng B, Obach RS, Burstein AH, Clark DJ, de Morais SM and Faessel HM. 2008. Effect of human renal cationic transporter inhibition on the pharmacokinetics of varenicline, a new therapy for smoking cessation: an in vitro-in vivo study. *Clin Pharmacol Ther.* 83(4):567-76.
- Graham FL, Smiley J, Russell WC and Nairn R. 1977. Characteristics of a human cell line transformed by DNA from Human Adenovirus Type 5. *J Gen Virol.* 36(59-72).
- Gorboulev V, Ulzheimer JC, Akhoundova A, Ulzheimer-Teuber I, Karbach U, Quester S, Baumann C, Lang F, Busch AE and Koepsell H. 1997. Cloning and characterization of two human polyspecific organic cation transporters. *DNA Cell Biol.* 16(7):871-81.
- Gorboulev V, Volk C, Arndt P, Akhoundova A and Koepsell H. 1999. Selectivity of the polyspecific cation transporter rOCT1 is changed by mutation of aspartate 475 to glutamate. *Mol Pharmacol.* 56(6):1254-61.
- Gorbunov D, Gorboulev V, Shatskaya N, Mueller T, Bamberg E, Friedrich T and Koepsell H. 2008. High-affinity cation binding to organic cation transporter 1 induces movement of helix 11

and blocks transport after mutations in a modeled interaction domain between two helices. *Mol Pharmacol.* 73(1):50-61.

Grover B, Auberger C, Sarangarajan R and Cacini W. 2002. Functional impairment of renal organic cation transport in experimental diabetes. *Pharmacol Toxicol.* 90(4):181-6.

Gründemann D, Gorboulev V, Gambaryan S, Veyhl M and Koepsell H. 1994. Drug excretion mediated by a new prototype of polyspecific transporter. *Nature.* 372(6506):549-52.

Gründemann D, Schechinger B, Rappold GA and Schömig E. 1998. Molecular identification of the corticosterone-sensitive extraneuronal catecholamine transporter. *Nat Neurosci.* 1(5):349-51.

Han TK, Everett RS, Proctor WR, Ng CM, Costales CL, Brouwer KL, Thakker DR. 2013. Organic cation transporter 1 (OCT1/mOct1) is localized in the apical membrane of Caco-2 cell monolayers and enterocytes. *Mol Pharmacol.* 84:182-9

Horvath G, Sutto Z, Torbati A, Conner GE, Salathe M and Wanner A. 2003. Norepinephrine transport by the extraneuronal monoamine transporter in human bronchial arterial smooth muscle cells. *Am J Physiol Lung Cell Mol Physiol.* 285(4):L829-37.

Ji L, Masuda S, Saito H and Inui K. 2002. Down-regulation of rat organic cation transporter rOCT2 by 5/6 nephrectomy. *Kidney Int.* 62(2):514-24.

Jung N, Lehmann C, Rubbert A, Knispel M, Hartmann P, van Lunzen J, Stellbrink HJ, Faetkenheuer G and Taubert D. 2008. Relevance of the organic cation transporters 1 and 2 for antiretroviral drug therapy in human immunodeficiency virus infection. *Drug Metab Dispos.* 36(8):1616-23.

Kaback HR, Dunten R, Frillingos S, Venkatesan P, Kwaw I, Zhang W, Ermolova N. 2007. Site-directed alkylation and the alternating access model for LacY. *Proc Natl Acad Sci* 104(2):491-4.

- Kekuda R, Prasad PD, Wu X, Wang H, Fei YJ, Leibach FH, Ganapathy V. 1998. Cloning and functional characterization of a potential-sensitive, polyspecific organic cation transporter (OCT3) most abundantly expressed in placenta. *J Biol Chem.* 273(26):15971-9.
- Keller T, Elfeber M, Gorboulev V, Reiländer H, Koepsell H. 2005. Purification and functional reconstitution of the rat organic cation transporter OCT1. *Biochemistry.* 44(36):12253-63.
- Keller T, Schwarz D, Bernhard F, Doetsch V, Hunte C, Gorboulev V, Koepsell H. 2008. Cell free expression and functional reconstitution of eukaryotic drug transporters. *Biochemistry.* 47(15):4552-64.
- Kimelblatt BJ, Cerra FB, Calleri G, Berg MJ, McMillen MA, Schentag JJ. 1980. Dose and serum concentration relationships in cimetidine-associated mental confusion. *Gastroenterology.* 78(4):791-5.
- Kimura H, Takeda M, Narikawa S, Enomoto A, Ichida K, Endou H. 2002. Human organic anion transporters and human organic cation transporters mediate renal transport of prostaglandins. *J Pharmacol Exp Ther.* 301(1):293-8.
- Kindla J, Fromm MF, König J. 2009. In vitro evidence for the role of OATP and OCT uptake transporters in drug-drug interactions. *Expert Opin Drug Metab Toxicol.* 5(5):489-500.
- Koepsell H, Schmitt BM, Gorboulev V. 2003. Organic cation transporters. *Rev Physiol Biochem Pharmacol.* 150:36-90.
- Koepsell H, Endou H. 2004. The SLC22 drug transporter family. *Pflugers Arch.* 447(5):666-76.
- Koepsell H. 2004. Polyspecific organic cation transporters: their functions and interactions with drugs. *Trends Pharmacol Sci.* 25(7):375-81.
- Koepsell H, Endou H. 2004. The SLC22 drug transporter family. *Pflugers Arch.* 447(5):666-76.
- Koepsell H, Lips K, Volk C. 2007. Polyspecific organic cation transporters: structure, function, physiological roles, and biopharmaceutical implications. *Pharm Res.* 24(7):1227-51.

- Koepsell H. 2011. Substrate recognition and translocation by polyspecific organic cation transporters. *Biol Chem.* 392(1-2):95-101.
- Koepsell H. 2013. The SLC22 family with transporters of organic cations, anions and zwitterions. *Mol Aspects Med.* 34(2-3):413-35.
- Koepsell H. 2015. Role of organic cation transporters in drug-drug interaction. *Expert Opin Drug Metab Toxicol.* 11(10):1619-33.
- Kusuhara H, Sugiyama Y. 2005. Active efflux across the blood-brain barrier: role of the solute carrier family. *NeuroRx.* 2(1):73-85.
- Lai MY, Jiang FM, Chung CH, Chen HC, Chao PD. 1988. Dose dependent effect of cimetidine on procainamide disposition in man. *Int J Clin Pharmacol Ther Toxicol.* 26(3):118-21.
- Lips KS, Volk C, Schmitt BM, Pfeil U, Arndt P, Miska D, Ermert L, Kummer W, Koepsell H. 2005. Polyspecific cation transporters mediate luminal release of acetylcholine from bronchial epithelium. *Am J Respir Cell Mol Biol.* 33(1):79-88.
- Lips KS, Wunsch J, Zarghooni S, Bschleipfer T, Schukowski K, Weidner W, Wessler I, Schwantes U, Koepsell H, Kummer W. 2007. Acetylcholine and molecular components of its synthesis and release machinery in the urothelium. *Eur Urol.* 51(4):1042-53.
- Lowry OH, Rosebrough NJ, Farr AL and Randall RJ. 1951. Protein measurement with the folin phenol reagent. *J Biol Chem.* 193(1): 265-275.
- Meijer DK, Mol WE, Mueller M, Kurz G. 1990. Carrier-mediated transport in the hepatic distribution and elimination of drugs, with special reference to the category of organic cations. *Journal of Pharmacokinetics and Biopharmaceutics.* 18(1):35-70.
- Meyer-Wentrup F, Karbach U, Gorboulev V, Arndt P, Koepsell H. 1998. Membrane localization of the electrogenic cation transporter rOCT1 in rat liver. *Biochem Biophys Res Commun.* 248(3):673-8.

- Moore KH, Yuen GJ, Raasch RH, Eron JJ, Martin D, Mydlow PK, Hussey EK. 1996. Pharmacokinetics of lamivudine administered alone and with trimethoprim-sulfamethoxazole. *Clin Pharmacol Ther.* 59(5):550-8.
- Motohashi H, Sakurai Y, Saito H, Masuda S, Urakami Y, Goto M, Fukatsu A, Ogawa O, Inui K. 2002. Gene expression levels and immunolocalization of organic ion transporters in the human kidney. *J Am Soc Nephrol.* 13(4):866-74.
- Müller J, Lips KS, Metzner L, Neubert RH, Koepsell H, Brandsch M. 2005. Drug specificity and intestinal membrane localization of human organic cation transporters (OCT). *Biochem Pharmacol.* 70(12):1851-60.
- Nagel G, Volk C, Friedrich T, Ulzheimer JC, Bamberg E, Koepsell H. 1997. A reevaluation of substrate specificity of the rat cation transporter rOCT1. *J Biol Chem.* 272(51):31953-6.
- Nies AT, Herrmann E, Brom M, Keppler D. 2008. Vectorial transport of the plant alkaloid berberine by double-transfected cells expressing the human organic cation transporter 1 (OCT1, SLC22A1) and the efflux pump MDR1 P-glycoprotein (ABCB1). *Naunyn Schmiedebergs Arch Pharmacol.* 376(6):449-61.
- Nies AT, Koepsell H, Winter S, Burk O, Klein K, Kerb R, Zanger UM, Keppler D, Schwab M, Schaeffeler E. 2009. Expression of organic cation transporters OCT1 (SLC22A1) and OCT3 (SLC22A3) is affected by genetic factors and cholestasis in human liver. *Hepatology.* 50(4):1227-40.
- Nies AT, Koepsell H, Damme K, Schwab M. 2011. Organic cation transporters (OCTs, MATes), in vitro and in vivo evidence for the importance in drug therapy. *Handb Exp Pharmacol.* (201):105-67.
- Nigam SK, Bush KT, Bhatnagar V. 2007. Drug and toxicant handling by the OAT organic anion transporters in the kidney and other tissues. *Nat Clin Pract Nephrol.* 3(8):443-8.

- Nishimura M, Yamaguchi M, Yamauchi A, Ueda N, Naito S. 2005. Role of soybean oil fat emulsion in the prevention of hepatic xenobiotic transporter mRNA up- and down-regulation induced by overdose of fat-free total parenteral nutrition in infant rats. *Drug Metab Pharmacokinet.* 20(1):46-54.
- Okuda M, Saito H, Urakami Y, Takano M, Inui K. 1996. cDNA cloning and functional expression of a novel rat kidney organic cation transporter, OCT2. *Biochem Biophys Res Commun.* 224(2):500-7.
- Okuda M, Urakami Y, Saito H, Inui K. 1999. Molecular mechanisms of organic cation transport in OCT2-expressing *Xenopus* oocytes. *Biochim Biophys Acta.* 1417(2):224-31.
- Owen MR, Doran E, Halestrap AP. 2000. Evidence that metformin exerts its anti-diabetic effects through inhibition of complex 1 of the mitochondrial respiratory chain. *Biochem J.* 348 Pt 3:607-14.
- Popp C, Gorboulev V, Müller TD, Gorbunov D, Shatskaya N, Koepsell H. 2005. Amino acids critical for substrate affinity of rat organic cation transporter 1 line the substrate binding region in a model derived from the tertiary structure of lactose permease. *Mol Pharmacol.* 67(5):1600-11.
- Rizwan AN, Burckhardt G. 2007. Organic anion transporters of the SLC22 family: biopharmaceutical, physiological, and pathological roles. *Pharm Res.* 24(3):450-70.
- Sekine T, Miyazaki H, Endou H. 2006. Molecular physiology of renal organic anion transporters. *Am J Physiol Renal Physiol.* 290(2):F251-61.
- Schmitt BM, Koepsell H. 2005. Alkali cation binding and permeation in the rat organic cation transporter rOCT2. *J Biol Chem.* 280(26):24481-90.
- Schmitt BM, Gorbunov D, Schlachtbauer P, Egenberger B, Gorboulev V, Wischmeyer E, Müller T, Koepsell H. 2009. Charge-to-substrate ratio during organic cation uptake by rat OCT2

is voltage dependent and altered by exchange of glutamate 448 with glutamine. *Am J Physiol Renal Physiol.* 296(4):F709-22.

Schneider E, Machavoine F, Pléau JM, Bertron AF, Thurmond RL, Ohtsu H, Watanabe T, Schinkel AH, Dy M. 2005. Organic cation transporter 3 modulates murine basophil functions by controlling intracellular histamine levels. *J Exp Med.* 202(3):387-93.

Tahara H, Kusuhara H, Endou H, Koepsell H, Imaoka T, Fuse E, Sugiyama Y. 2005. A species difference in the transport activities of H₂ receptor antagonists by rat and human renal organic anion and cation transporters. *J Pharmacol Exp Ther.* 315(1):337-45.

Tanihara Y, Masuda S, Katsura T, Inui K. 2009. Protective effect of concomitant administration of imatinib on cisplatin-induced nephrotoxicity focusing on renal organic cation transporter OCT2. *Biochem Pharmacol.* 78(9):1263-71.

Taubert D, Grimberg G, Stenzel W, Schömig E. 2007. Identification of the endogenous key substrates of the human organic cation transporter OCT2 and their implication in function of dopaminergic neurons. *PLoS One.* 2(4):e385.

Thévenod F¹, Ciarimboli G, Leistner M, Wolff NA, Lee WK, Schatz I, Keller T, Al-Monajjed R, Gorboulev V, Koepsell H. 2013. Substrate- and cell contact-dependent inhibitor affinity of human organic cation transporter 2: studies with two classical organic cation substrates and the novel substrate cd²⁺. *Mol Pharm.* 10(8):3045-56.

Tzvetkov MV, Vormfelde SV, Balen D, Meineke I, Schmidt T, Sehrt D, Sabolić I, Koepsell H, Brockmüller J. 2009. The effects of genetic polymorphisms in the organic cation transporters OCT1, OCT2, and OCT3 on the renal clearance of metformin. *Clin Pharmacol Ther.* 86(3):299-306.

Umehara KI, Iwatsubo T, Noguchi K, Usui T, Kamimura H. 2008. Effect of cationic drugs on the transporting activity of human and rat OCT/Oct 1-3 in vitro and implications for drug-drug interactions. *Xenobiotica.* 38(9):1203-18.

- Van Crugten J, Bochner F, Keal J, Somogyi A. 1986. Selectivity of the cimetidine-induced alterations in the renal handling of organic substrates in humans. Studies with anionic, cationic and zwitterionic drugs. *J Pharmacol Exp Ther.* 236(2):481-7.
- Verhaagh S, Schweifer N, Barlow DP, Zwart R. 1999. Cloning of the mouse and human solute carrier 22a3 (Slc22a3/SLC22A3) identifies a conserved cluster of three organic cation transporters on mouse chromosome 17 and human 6q26-q27. *Genomics.* 55(2):209-18.
- Volk C, Gorboulev V, Budiman T, Nagel G, Koepsell H. 2003. Different affinities of inhibitors to the outwardly and inwardly directed substrate binding site of organic cation transporter 2. *Mol Pharmacol.* 64(5):1037-47.
- Volk C, Gorboulev V, Kotzsch A, Müller TD, Koepsell H. 2009. Five amino acids in the innermost cavity of the substrate binding cleft of organic cation transporter 1 interact with extracellular and intracellular corticosterone. *Mol Pharmacol.* 76(2):275-89.
- Walsh DR, Nolin TD and Friedman PA. 2015. Drug Transporters and Na⁺/H⁺ Exchange Regulatory Factor PSD-95/Drosophila Discs Large/ZO-1 Proteins. *Pharmacological Reviews.* 67 (3) 656-680.
- Wang DS, Kusuhara H, Kato Y, Jonker JW, Schinkel AH, Sugiyama Y. 2003. Involvement of organic cation transporter 1 in the lactic acidosis caused by metformin. *Mol Pharmacol.* 63(4):844-8.
- Wang ZJ, Yin OQ, Tomlinson B, Chow MS. 2008. OCT2 polymorphisms and in-vivo renal functional consequence: studies with metformin and cimetidine. *Pharmacogenet Genomics.* 18(7):637-45.
- Wright SH, Dantzler WH. 2004. Molecular and cellular physiology of renal organic cation and anion transport. *Physiol Rev.* 84(3):987-1049.

Zaïr ZM, Eloranta JJ, Stieger B, Kullak-Ublick GA. 2008. Pharmacogenetics of OATP (SLC21/SLCO), OAT and OCT (SLC22) and PEPT (SLC15) transporters in the intestine, liver and kidney. *Pharmacogenomics*. 9(5):597-624.

Zolk O, Solbach TF, König J, Fromm MF. 2009. Functional characterization of the human organic cation transporter 2 variant p.270Ala>Ser. *Drug Metab Dispos*. 37(6):1312-8.

Zwart R, Verhaagh S, Buitelaar M, Popp-Snijders C, Barlow DP. 2001. Impaired activity of the extraneuronal monoamine transporter system known as uptake-2 in Orct3/Slc22a3-deficient mice. *Mol Cell Biol*. 21(13):4188-96.

10. Acknowledgements

I would like to express my heartfelt gratitude to my supervisor Prof. Hermann Koepsell for giving me the superb opportunity of working in his institute and for encouraging me to complete my work despite the difficult nature of my situation. His expertise, understanding and generous guidance and support added considerably to my experience. I consider him my mentor!

I am also grateful to my co-supervisors, Prof. Thomas Mueller and Prof. Erhard Wischmeyer for their valuable inputs during the annual reviewing conducted on behalf of Graduate School of Life Sciences (GSLs).

I would also like to thank GSLs for allowing me to complete my PhD after such a long gap and providing a very wholesome environment to me as an enrolled student by conducting various curriculum activities and international outreach programs. It added a lot to my exposure!

I am indebted to Dr. Rose Liebert, Dr. Gabrielle Blum-Oehler, Dr. George Leigh and Mrs. Jennifer Braysher for their generous advice and help in matters of procedures regarding the GSLs activities and thesis submission.

I am thankful to the funding organization *Deutsche Forschungsgemeinschaft* (DFG) and *DAAD-Stipendien und Betreuungsprogram* (STIBET) for providing monetary support during my PhD thesis.

I am immensely thankful to Dr. Valentin Gorboulev for reviewing my thesis and for his unlimited support throughout my PhD work till the point of submitting the thesis.

I am also grateful to Mrs. Ursula Roth and Mrs. Brigitte Duerner for teaching me the techniques.
Vielen Dank, dass ihr beide für mich geduldig seid!

I would also like to express heartfelt thanks to Mr. Michael Christof for his generous help in constructing graphs.

Thank you Mrs. Grabandt, Mrs. Irina Schatz, Mrs. Elke Varin, Mrs. Alla Ganscher, Mr. W Axt and Mr. H Eichelmann for your help in administrative and technical matters.

I am thankful to my colleagues Dr. Volk, Dr. Keller, Dr. Kipp, Maike, Biggie, Alina, Chakri, Prashant, Alex for providing a very rich and nice environment in the lab which allowed me to give my best.

A very special thanks goes to:

Aruna, for her invaluable companionship throughout my stay in Germany and for still being right beside me round the clock despite the distance!

Shruti, for helping me adjust in an alien city when I first stepped there.

Kushal, for his motivation and for helping me reconnect with Wuerzburg.

Priya, for being the wholesaler of excellent ideas.

Neha, for being my emotional support during the time I needed it the most.

Manish, for making things light.

Hemant, for readily helping a stranger.

Thank you all of you for providing me with a home away from home!

Shikeb, for being my brother and the best software engineer and Hina for the encouraging words.

Naushin, for behaving like my elder sister instead of the younger one and for the tough babysitting job and Zimnish, Shahwaz and Fareha for engaging my toddlers!

My parents, for their unconditional and unending support in every sphere of life and my in-laws, for understanding and cooperating with me.

My husband, Naved, for being my best friend and for tolerating my impulsiveness all the time.

My daughters, Zainab and Ayesha, for being the reason I completed my PhD.

11. Curriculum vitae

Name: Saba Rehman
 Date of Birth: March 11, 1981
 Place of Birth: New Delhi, India
 Citizenship: Indian

Education:

Aug 1999 – Jul 2002	B.Sc. Bioscience <i>Jamia Millia Islamia, New Delhi, India</i>
Aug 2002 – Jul 2003	B.Ed. (Bachelor of Education) <i>Jamia Millia Islamia, New Delhi, India</i>
Aug 2003 – Jul 2005	M.Sc. Biotechnology <i>Jamia Millia Islamia, New Delhi, India</i>
Jan 2005 – Jun 2005	Masters Dissertation Student <i>National Institute of Immunology (NII), New Delhi, India</i> Supervisor: Dr. Rajni Rani
Jan 2006 – Feb 2008	Post Graduate Teacher (PGT) Biotechnology <i>Hamdard Public School, New Delhi, India</i>
Mar 2009 – Dec 2011	Ph.D. Student, Scientific Co-worker <i>Graduate School of Life Sciences, Institute for Anatomy and Physiology, University of Wuerzburg, Wuerzburg, Bavaria, Germany</i> Primary Supervisor: Prof. Dr. Hermann Koepsell
Jan 2012 – Dec 2016	<i>Sabbatical</i> due to Marriage and Kids
Jan 2017 – Dec 2017	Thesis writing and submission <i>Graduate School of Life Sciences, Institute for Anatomy and Physiology, University of Wuerzburg, Wuerzburg, Bavaria, Germany</i> Primary Supervisor: Prof. Dr. Hermann Koepsell

12. Publication

Assay Conditions Influence Ligand Affinities of Rat Organic Cation Transporter 1: Analysis of Mutagenesis in the Modeled Outward-facing Cleft Measuring Ligand Effects on Initial Uptake.

Valentin Gorboulev, Saba Rehman, Christoph Michael Albert, Ursula Roth, Marleen Julia Meyer, Mladen Vassielev Tzvetkov, Thomas Dieter Mueller, and Hermann Koepsell

MOLPHARM/2017/110767 (*Revised version under review*)

13. Participation in international scientific conferences

- Rehman S, Koepsell H. Identification of accessible and closed substrate binding sites in the outward open cleft of rat organic cation transporter 1.
Presented at: *5th International Symposium – “Chiasma” (October 13-14, 2010)*
Graduate School of Life Sciences (GSLs), Wuerzburg, Germany.
- Rehman S, Koepsell H. Identification of accessible and closed substrate binding sites in the outward open cleft of rat organic cation transporter 1.
Presented at: *The International Symposium – “Molecular Pharmacology of Receptors, Channels and Transporters”, (July 28-30, 2011)*
Rudolf Virchow Centre, University Clinic, Wuerzburg, Germany.
- Rehman S, Koepsell H. Identification of accessible and closed substrate binding sites in the outward open cleft of rat organic cation transporter 1.
Presented at: *The International Symposium – “An Integrated Approach to the Physiology of Organic Cation Transporters”, (October 15-16, 2010)*
Institute of Physiology, Dept of Vegetative Physiology, Georg-August-Universität, Goettingen, Germany.

Affidavit

I hereby confirm that my thesis entitled "**Identification of accessible and closed substrate-binding sites in the outward open cleft of rat organic cation transporter (rOCT1)**" is the result of my own work. I did not receive any help or support from commercial consultants. All sources and/or materials applied are listed and specified in the thesis.

Furthermore, I confirm that this thesis has not yet been submitted as part of another examination process, neither in identical nor in similar form.

New Delhi (India)

Signature

Eidesstattliche Erklärung

Hiermit erkläre ich an Eides statt, die Dissertation "**Identifizierung von zugänglichen und unzugänglichen Substratbindungsstellen in der nach außen offenen Konformation des organischen Kationentransporters rOCT1**" eigenständig, d.h. insbesondere selbständig und ohne Hilfe eines kommerziellen Promotionsberaters, angefertigt und keine anderen als die von mir angegebenen Quellen und Hilfsmittel verwendet zu haben.

Ich erkläre außerdem, dass die Dissertation weder in gleicher noch in ähnlicher Form bereits in einem anderen Prüfungsverfahren vorgelegen hat.

Neu Delhi (Indien)

Unterschrift